

Emily Larsen Cosgriff

Modeling, Simulation and Control of a CO₂ Heat Pump and Heating Facility

Master's thesis in Industrial Cybernetics

Supervisor: Lars Imsland

June 2023

Emily Larsen Cosgriff

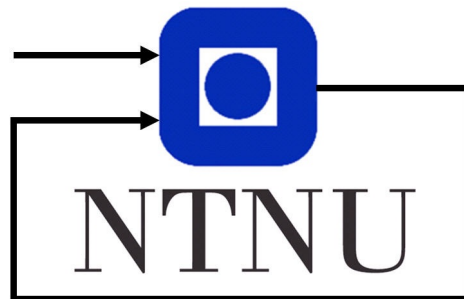
Modeling, Simulation and Control of a CO₂ Heat Pump and Heating Facility

Master's thesis in Industrial Cybernetics
Supervisor: Lars Imsland
June 2023

Norwegian University of Science and Technology
Faculty of Information Technology and Electrical Engineering
Department of Engineering Cybernetics



Modeling, Simulation and Control of a CO₂ Heat Pump and Heating Facility



Author:
Emily Larsen Cosgriff

Supervisor:
Lars Imsland

Master's thesis
Department of Engineering Cybernetics
Norwegian University of Science and Technology

June 8, 2023

Preface

This thesis has been written as a concluding part of the master's program in Industrial Cybernetics at the Department of Engineering Cybernetics, at the Norwegian University of Science and Technology (NTNU). The project is written for NTNU, and is based on the specialization project, TTK4551, which was completed in the fall of 2022. The thesis provides a thorough description of model building in Simulink, from developing an RC model of a heating facility, to modeling the transcritical CO₂ heating cycle. These models aim to simulate the temperature dynamics of the heating facility and investigate the effectiveness of temperature control through the implementation of controllers. The work presented in this thesis has been conducted independently, with academic support from NTNU's Department of Engineering Cybernetics and the Department of Energy and Process Engineering.

I want to thank my supervisor, Lars Imsland, for his guidance throughout this project. I would also like to thank Natasa Nord at the Department of Energy and Process Engineering for her contributions to this work.

Emily Larsen Cosgriff
Trondheim, June 8, 2023

Abstract

Increased energy costs and growing environmental concerns have prompted a search for energy-efficient and cost-effective heating solutions. Carbon dioxide (CO₂) heat pumps have emerged as a more environmentally friendly option compared to the ozone depleting traditional refrigerants like chlorofluorocarbons and hydrofluorocarbons. Despite extensive research on the use of CO₂ as a refrigerant, the exploration of automatic control strategies for enhancing accuracy and efficiency of heating systems is yet to be addressed.

This thesis presents a comprehensive investigation into the effectiveness of Proportional-Integral-Derivative (PID) and Model Predictive Control (MPC) strategies for temperature regulation in a CO₂ heat pump system and its connected heating facility. The study aims to compare the performance of these control methods and determine their suitability for practical applications. To achieve this, a simulation framework was developed using Matlab and Simulink. An RC model of the heating facility was constructed and connected to two different models: a simplified radiator model and a more complex CO₂ heat pump cycle model. The PID and MPC control strategies were implemented on both models, allowing for a direct comparison of their performance in regulating the temperature within the facility.

The simulation results revealed that the MPC control strategy exhibited superior temperature tracking capabilities compared to PID. The MPC controller demonstrated precise temperature control, ensuring the desired setpoint temperature was consistently maintained. Conversely, the PID controller showcased satisfactory performance in temperature regulation, indicating its potential suitability for controlling temperatures in residential homes. The simplicity and ease of implementation associated with PID controllers make them a practical choice for residential applications, where precise temperature control may not be as critical.

These findings provide valuable insights into the selection of appropriate control strategies for temperature regulation in CO₂ heat pump systems. The research contributes to the understanding of PID and MPC control methods, their strengths, and their limitations. Furthermore, the development of thermal building models contributes to the understanding of energy dynamics, heat transfer processes, and the optimization of Heating, Ventilation, and Air Conditioning (HVAC) systems. The results can guide future efforts in optimizing control strategies for enhanced energy efficiency and improved comfort in residential heating systems.

Sammendrag

Økte energikostnader og økende bekymring for miljøet har ført til et behov for energi- og kostnadseffektive oppvarmingsløsninger. Karbondioksid (CO_2) varmepumper er et mer miljøvennlig alternativ sammenlignet med tradisjonelle kjølemedier som klorfluorkarboneer og hydrofluorkarboneer, som bidrar til ozonlagets nedbrytning. Til tross for omfattende forskning på bruken av CO_2 som kjølemedium, er det fremdeles behov for å utforske automatiske kontrollstrategier for å forbedre nøyaktighet og effektivitet i oppvarmingssystemer.

Denne masteroppgaven presenterer en omfattende undersøkelse av effektiviteten til Proporsjonal-Integral-Derivasjon (PID) og Model Predictive Control (MPC) strategier for temperaturregulering i et CO_2 -basert varmepumpeanlegg og dets tilhørende oppvarmingsanlegg. Studien har som mål å sammenligne ytelsen til disse reguleringsmetodene og bestemme deres egnethet for praktiske anvendelser. For å oppnå dette ble det utviklet en simuleringsplattform ved hjelp av Matlab og Simulink. En RC-modell av oppvarmingsanlegget ble konstruert og koblet til to forskjellige modeller: en forenklet radiator-modell og en mer kompleks CO_2 -varmepumpe-syklusmodell. PID- og MPC-reguleringsstrategiene ble implementert på begge modellene, noe som muliggjorde en direkte sammenligning av deres ytelse i temperaturreguleringen i oppvarmingsanlegget.

Simuleringsresultatene avdekket at MPC-reguleringsstrategien hadde overlegne evner til å følge temperaturendringer sammenlignet med PID-regulering. MPC-regulatoren viste presis temperaturkontroll og sikret at ønsket temperaturmål ble opprettholdt. PID-regulatoren viste tilfredsstillende ytelse i temperaturreguleringen, noe som indikerer potensialet for bruk i temperaturregulering i bolighus. PID-regulatorens enkle oppbygning og implementering gjør dem til et praktisk valg for boligapplikasjoner der rask og presis temperaturregulering ikke er kritisk.

Disse funnene gir verdifull innsikt i valget av egnede kontrollstrategier for temperaturregulering i CO_2 -varmepumpesystemer. Forskningen bidrar til forståelsen av PID- og MPC-kontrollmetoder, inkludert deres styrker og begrensninger. Videre bidrar utviklingen av termiske bygningsmodeller til økt forståelse av energidynamikk, varmeoverføringsprosesser og optimalisering av HVAC-systemer. Resultatene kan veilede fremtidige tiltak for å optimalisere kontrollstrategier, med sikte på å forbedre energieffektivitet og øke komforten i boligoppvarmingssystemer.

Table of Contents

Preface	i
Abstract	ii
Sammendrag	iii
List of Tables	vii
List of Figures	ix
Abbreviations	x
1 Introduction	1
1.1 Background and Motivation	1
1.2 Literature Review	2
1.2.1 RC Models	2
1.2.2 PID Controller Tuning in HVAC Systems	3
1.2.3 MPC in HVAC Systems	3
1.3 Problem Description	4
1.4 Delimitations	5
1.5 Structure of the Report	5
2 System Description	7
2.1 Heat Transfer	7
2.2 Heat Pump Cycle	8
2.2.1 Transcritical CO ₂ Heat Pump Cycle	8
2.3 Heating Facility	10
3 Modeling	13
3.1 Modeling Paradigms	13
3.2 Conservation Laws	14
3.3 Thermal-electrical Analogy	15

3.4	Modeling a Room	16
3.4.1	3R2C Model	17
3.4.2	Modeling the Walls and Ceiling	18
3.4.3	Modeling the Floor	18
3.4.4	Modeling the Window	18
3.4.5	Room Model	19
3.5	Verification of the Room Model	20
3.6	Modeling the CO ₂ Cycle	22
4	Automatic Control	24
4.1	PID Control	25
4.1.1	Tuning Methods	26
4.2	Model Predictive Control	27
4.2.1	MPC Toolbox in Matlab	28
5	Controller Implementation	32
5.1	Implementation for the Simplified Radiator	32
5.1.1	Implementation of PID in Simulink	32
5.1.2	Implementation of MPC in Simulink	33
5.2	Implementation for the CO ₂ Cycle	36
5.2.1	PID Controller Parameters	36
5.2.2	MPC Controller Parameters	37
6	Results	40
6.1	Temperature Control Using the Simplified Radiator	40
6.1.1	Control of Temperature with PID	40
6.1.2	Control of Temperature with MPC	41
6.2	Temperature Control with the CO ₂ Cycle	42
6.2.1	PID Control of the Room Temperature	42
6.2.2	Control of Room Temperature with MPC	43
7	Discussion	45
7.1	Controller Comparison	45
7.2	Limitations	46
7.2.1	Simplified Assumptions	46
7.2.2	Considerations for Controller Parameter Selection	47
7.2.3	Equipment Sizing	48
7.2.4	Generalizability	48
8	Conclusion	49
8.1	Further Work	49
	Bibliography	51

Appendix		55
A	Matlab files	55
B	Modeling Ventilation and Infiltration	57
C	PID Tuning Methods	58

List of Tables

3.1	Thermal-Electrical Analogy	16
3.2	Typical values of convective heat transfer coefficients in buildings. Values found in [37]	19
3.3	Typical values of overall heat transfer coefficients in building elements. Values found in [38]	20
4.1	Effect of increasing the individual controller parameters.	27
5.1	Controlled, manipulated, and disturbance variables in the system.	32
A.1	Tuning relations for the Z-N method [44]	58

List of Figures

2.1	Schematic of a General Heat Pump System	8
2.2	Pressure-Enthalpy diagram for trans-critical CO ₂ heat pump. Figure from [30]	9
2.3	Process diagram of the heat pump cycle	11
2.4	Process diagram of the heating facility	12
3.1	Overview of typical features of the three modeling paradigms. Figure from [16]	15
3.2	3R2C model	17
3.3	Model of the floor	18
3.4	Model of the window	18
3.5	Simulink/Simscape model of the room	19
3.6	Room temperature development over 24 hours, with outdoor temperature at 5°C, initial wall temperature at 10°C, and initial indoor temperature at 20°C.	21
3.7	Room temperature development over 24 hours, with the outdoor temperature fluctuating between 2 and 7°C, initial wall temperature at 10°C, and initial indoor temperature at 20°C.	21
3.8	Simulink model of transcritical CO ₂ heat pump cycle	22
4.1	Block diagram of parallel PID controller. Figure from [33]	25
4.2	Block diagram of the MPC control scheme. Figure from [33]	28
4.3	General concept of the MPC control scheme. Figure from [33]	29
4.4	Model structure used in an MPC controller. Figure from [42]	30
5.1	Simulink model of room with PID control to regulate the temperature of the radiator	33
5.2	Simulink model of the room with MPC	34
5.3	Simulink model of CO ₂ heating cycle with heating facility	37
5.4	Simulink model of the CO ₂ heating cycle with MPC control	39

6.1	Step response of the development of the room temperature over one hour using a PID controller to control the radiator temperature. ($K_p = 40, K_i = 0.1, K_d = 0$)	41
6.2	Step response of the development of the room temperature over one hour using MPC to control the radiator temperature.	42
6.3	Step response of the development of the room temperature over one hour using PID to control the shaft speed of the compressor. ($K_p = 1000, K_i = 2, K_d = 0$)	43
6.4	Step response of the development of the room temperature over one hour using an MPC controller to control the compressor speed.	44
7.1	Simulink model of the simplified heat exchange between the CO ₂ cycle and the water loop heating up the room	48
8.1	Process reaction curve for a first-order-plus-time-delay model [33]	59

Abbreviations

Abbreviation	Description
CFCs	Chlorofluorocarbons
COP	Coefficient of performance
CFD	Computational fluid dynamics
CV	Controlled variable
DHW	Domestic hot water
DV	Disturbance variable
FOPTD	First-order-plus-time-delay
GWP	Global warming potential
HFCs	Hydrofluorocarbons
HVAC	Heating, Ventilation, and Air Conditioning
LTi	Linear-time-invariant
MD	Measured disturbance
MO	Measured output
MPC	Model predictive control
MV	Manipulated variable
OV	Output variable
PID	Proportional Integral Derivative
QP	Quadratic program
RMSE	Root-mean-square error
SIMC	Simple Internal Model Control
Z-N	Ziegler-Nichols

1

Introduction

1.1 Background and Motivation

Energy consumption is becoming an increased concern for most households. Both the growing concern for global warming and the high energy prices are incentives to increase energy efficiency in residential buildings. The United States Environmental Protection Agency states that space heating accounts for 42% of residential energy usage [1]. Reducing the energy consumption for residential heating is essential for cost and energy savings.

Heat pump systems are a common way of heating residential buildings. According to the Norwegian Water Resources and Energy Directorate [2], heat pump systems are delivering about 15 TWh of heat, and it is expected that they will continue to increase the heat delivery to 18-20 TWh by 2030. This effect is distributed around about 750 000 heat pumps currently operating in the country. Although installing heat pumps can be expensive compared to electrical heaters, using the heat pumps are much more energy effective than the electrical alternative. Heat pumps allow for generating heat from low-temperature sources such as outdoor air or water. Using heat pumps instead of electrical heaters reduces the power load by 1 GW on a cold winter day. Furthermore, all heat demand in buildings could in theory be supplied by heat pumps. Continuous development and research on heat pumps are therefore important for optimizing the technology.

The use of traditional refrigerants in heat pumps, such as chlorofluorocarbons (CFCs) and hydrofluorocarbons (HFCs), has been shown to have harmful effects on the ozone layer. To mitigate this, CO₂ is being used as an alternative refrigerant, which is more environmentally friendly. CFCs and HFCs used to be the preferred refrigerants over CO₂ due to their improved heating and cooling properties. However, following the Montreal Protocol's ban on ozone-depleting refrigerants [3], the search for alternative refrigerants intensified. Although many natural refrigerants exist, only a few meet the necessary technical and safety standards [4]. Among these, CO₂ stands out as a safe and suitable option since it is non-toxic and non-flammable, and has a low global warming potential (GWP) of 1, compared to the high GWP of HFCs (up to 3000 times greater than CO₂ per kilogram) [5]. Moreover, CO₂ is economically accessible as it is a byproduct of industrial processes

with a net zero global impact. In the past two decades, researchers have made progress in investigating the use of CO₂ as a refrigerant, but there is still a need for more efficient automatic control methods around the heat pump system.

Efficient automatic control methods in HVAC systems are investigated by creating dynamic models of buildings and control methods and simulating their behavior. Thermal modeling and simulation are essential components of this process, enabling the understanding and prediction of system behavior over time. By utilizing mathematical equations, these techniques allow for experimentation and analysis of complex systems that may be challenging to study in real-world settings. In thermal modeling, the thermal properties of building elements are considered, allowing for the estimation of thermal resistance and capacitance for each element. This approach, known as RC modeling, utilizes resistors and capacitors to represent thermal elements. The combination of modeling and simulation not only supports hypothesis testing, controller optimization, and informed decision-making, but also provides valuable insights into system responses under different operating conditions.

1.2 Literature Review

This section is a review of the literature on RC building models and automatic control of HVAC systems, highlighting the major findings, methodologies, and theories that have shaped the field. Gaps and limitations in the literature will also be discussed, identifying areas for further research and potential contributions to the field. By examining the existing literature, this review aims to provide a comprehensive understanding of the topic and inform future research and practice.

1.2.1 RC Models

RC modeling involves combining the building elements of high thermal mass into one or more capacitors. The number of capacitors used is the order of the model. E.g. using a single capacitor is a first-order representation, while using two capacitors is a second-order representation. Naturally, the more capacitors used, the more complex the RC model becomes. Using a combination of first and second-order representations to model buildings have been proven to give good agreement between the model and the true measurements. Achterbosch et.al. [6] used a second-order representation to model the external wall and floor, while the windows, ceilings, and partitions were modeled using a first-order representation, and the model was a good representation of the actual building. The model was tested on houses with different construction materials and hence different thermal capacities, yet the model was able to estimate the temperature development of the physical houses accurately. Higher-order representations are commonly used in models but tend to be used in more complicated thermal systems. Third-ordered representations were used by Lefebvre to model buildings [7], and by Mara et.al. to model a passive solar cell [8]. Fourth-order representations were used by Fraisse et.al to model a multi-layer wall in a building. Yet, a second-order model was used by Underwood where 45 construction elements were included, showing that the model is showing excellent agreement with the reference[9].

These findings suggest that RC modeling is an effective way to represent the thermal properties of buildings and can be adapted for various types of constructions. Despite certain drawbacks such as simplifying complex building systems and the need for higher-ordered models to represent complicated thermal systems, the methodologies discussed have played a significant role in advancing RC modeling as a valuable tool for thermal modeling of buildings.

1.2.2 PID Controller Tuning in HVAC Systems

While there is a lack of specific research on systematic tuning of PID controllers for optimizing energy efficiency in CO₂ HVAC systems, prior studies have provided valuable insights into the automatic control of such systems. Researchers such as Zhou et al. have developed fuzzy PID controllers for CO₂ heat pump systems using the Ziegler-Nichols method, demonstrating that PID is a viable control strategy [10]. Kasahara et al. compared different tuning methods for PID controllers in HVAC systems and found that the Ziegler-Nichols method produced satisfactory but oscillatory responses [11]. Clauß et al. highlighted the common use of Ziegler-Nichols and Skogestad methods for controller tuning when manufacturer parameters are unavailable [12]. Additionally, Xu et al. employed trial-and-error techniques to determine optimal PID controller settings for a transcritical CO₂ electric vehicle heat pump [13]. While further research is needed to address the specific challenges of optimizing CO₂ heat pump systems' energy efficiency through PID controller tuning, these prior studies offer valuable starting points and insights for future investigations.

1.2.3 MPC in HVAC Systems

In recent years, MPC has emerged as an effective method for controlling HVAC systems. Many studies have shown that MPC can effectively control heat pump systems, providing optimal control strategies, especially in terms of energy efficiency. For instance, Kim et al. used MPC to control a ground-source heat pump system and found that it improved the system's performance by reducing energy consumption and maintaining the desired temperature set-point [14]. A study by Yang et al. showed that MPC could be used to control the operation of an air-to-water heat pump system by adjusting the heating capacity and flow rate, leading to a significant reduction in energy consumption [15].

MPC problems are classified into three main problem classes - linear, nonlinear, and hybrid. A complete overview and unified framework of MPC control in HVAC control applications has been conducted by Drgoña et. al. and is found in [16]. In the review, it was found that linear MPC formulation is the simplest and computationally least demanding to implement. It is commonly used in the building sector because linear dynamics can accurately represent the building envelope [17]. Nonlinear MPC offers greater flexibility and potentially improved performance by incorporating nonlinear HVAC models, but it requires more complex modeling and increased computational resources. Studies such as [18, 19, 20] show how nonlinear MPC is used in real applications. Hybrid MPC is useful when dealing with integer decision variables or switching dynamics, which are common in building applications. Although hybrid MPC requires more computational resources, it can offer better performance compared to linear MPC [21].

Drgoňa et. al. [16] also reviewed common algorithmic solutions of MPC and found that the three solution techniques, namely implicit, explicit, and approximate MPC, have both advantages and disadvantages. Building climate control applications have specific characteristics such as a large number of state variables and slow dynamics, which make online implicit MPC implementation the most common approach. However, this method requires computational power and software dependencies [22]. Explicit MPC is feasible for small case studies (seen in [23]) and suitable for low-level control tasks or decentralized single-zone control strategies [24]. Approximate explicit MPC solutions offer memory-based control policies with low computational footprints, making them promising for large-scale problems. They require minimal software dependencies and can operate on lower-level hardware. The drawback is the need for the original MPC and larger training datasets. The paper also addresses uncertainties in the MPC problem and methods like offset-free MPC, robust MPC, stochastic MPC, adaptive MPC, and learning-based MPC for mitigating them.

The existing literature includes studies comparing different MPC formulations, modeling methods, and tools to assess MPC performance. However, there is a lack of a unified framework that specifically addresses the challenges in evaluating and assessing MPC performance. Most of the literature is constrained to specific implementations and conditions in which they were compared, while the tools are limited to the building models and MPC approaches developed by the tool designers [16]. Furthermore, real implementations of MPC in buildings are often short-term studies, as they are often simulated for hours or days, instead of years [16]. It hinders the ability to assess long-term maintenance requirements. Additionally, there is a lack of studies that discuss implementation costs and payback periods. Another challenge lies in defining the criteria for comparison. While common metrics like energy savings, operating cost reductions, and improved occupant comfort are used, there are other important factors to consider, such as computer hardware and software requirements, computation time, robustness to changing conditions, sensitivity to model and forecast uncertainties, data requirements, implementation effort, and installer expertise as discussed in [16]. The wide range of these factors makes it difficult to make objective comparisons.

Despite the gaps and limitations in the literature, the use of MPC in HVAC systems has proven to be effective in optimizing system performance and reducing energy consumption. The studies on this topic have employed various approaches, including system modeling and optimization algorithms, to achieve these results. As the demand for energy-efficient HVAC systems continues to grow, the use of MPC is likely to become more prevalent, leading to further advancements in the field.

1.3 Problem Description

Traditional refrigerants like CFCs and HFCs used in heat pump systems contribute to ozone layer depletion when released into the atmosphere. To mitigate environmental harm, CO₂ has emerged as a more eco-friendly alternative for heating processes. Efficient control strategies can significantly impact the overall energy efficiency and performance of the system. Using effective controllers in CO₂-based heat pumps is therefore crucial for optimizing energy usage.

This project is a continuation of the semester project [25], where PID controllers for a CO₂ heat pump with a connected heating facility, located in the laboratory at the Department of Energy and Process Engineering were attempted to be tuned. However, none of the controllers were successfully tuned due to inaccurate temperature sensors and errors in the software implementation. As a result, instead of working on the physical system, this thesis involves developing mathematical models of the heat pump and heating facility. By developing mathematical models of the system, software programs like Simulink can be used to simulate the behavior of the system over time.

The aim of this project is to investigate the performance of PID and MPC controllers to regulate the room temperature inside the heating facility. To achieve this, an RC model of the heating facility (referred to as the room) is developed and connected to both a simplified model of the radiator and a model of the complete CO₂ heat pump cycle. The performance of the two controllers is then compared, and quantitative methods are employed to determine the optimal controller settings.

1.4 Delimitations

This project is delimited to focus solely on the modeling and simulation of the transcritical CO₂ heat pump cycle and the connected heating facility. The emphasis is on studying the temperature development of the room by employing PID and MPC controllers to regulate the output of a radiator. The project does not address the implementation or tuning of the physical controllers used in the system. It should be noted that the equipment sizing employed in the simulations does not accurately represent real-world equipment sizes. The mathematical models developed in this project are general and can be applied to a wide range of buildings. However, they are limited by constants and parameters specific to the simulated heating facility.

1.5 Structure of the Report

The following paragraphs briefly describe the structure of the report. Chapter 2 is meant to give a short recap on the thermodynamics of heat transfer before a general heat pump cycle is described. Although all heat pumps have four primary components, CO₂ heat pumps possess an additional internal heat exchanger, which will be thoroughly explained. The final section of the chapter explains the physical setup of the heat pump cycle and the heating facility that is to be modeled.

In Chapter 3, a mathematical model of the heating facility is derived from the laws of thermodynamics and by using the thermal-electrical analogy. The different elements of the room are modeled individually before all elements are connected to make up the room model. The room model is then verified by simulating the temperature development of the indoor air with no added heat in Simulink. Lastly, a model of the transcritical CO₂ heat pump cycle is presented and described. An example model from MathWorks is modified to be used as the transcritical CO₂ cycle.

Chapter 4 concerns the two automatic controllers used in this project. The PID and MPC controllers are described in this chapter. Theory for controller tuning is also included,

as well as a description of how the MPC toolbox in Matlab works.

In Chapter 5, the two automatic controllers are implemented into the Simulink model. The first section of the chapter involves the implementation of the controllers used in the simplified radiator model (e.g. not modeling the CO₂ heat pump cycle), while the second section regards the CO₂ cycle implementation. The selection of controller parameters for the PID and MPC are presented.

The results of this project are presented in Chapter 6. The chapter is divided into two sections, where the first section presents temperature development using a simplified radiator, and the last section presents the same type of response plots but the radiator gain is modeled using the transcritical CO₂ cycle. Plots of the controller outputs and temperature development are presented.

A discussion of the results is done in Chapter 7. Limitations of the models used are discussed. Chapter 8 is the conclusion of this thesis, and suggestions for further work are also included in this chapter.

2

System Description

In this chapter, the heat pump cycle and heating facility of the physical system are described. However, before the system is introduced, the basic theory behind heat transfer and pumps is presented. Having an understanding of how the heat pump cycle works is beneficial in understanding how buildings are heated up. The following paragraphs are intended to give a short refresher on thermodynamics, in addition to explaining how a general heat pump works. The end of this chapter explains the physical setup of the heat pump cycle and the heating facility. Large parts of this chapter are based on the theory and methods presented in the specialization project [25].

2.1 Heat Transfer

Exchanging heat between flowing streams, whether it is between solids, liquids, or gases is done through a heat exchanger. While heat exchangers can exist in various configurations, they all rely upon the fundamental principles of heat transfer, specifically conduction, convection, and radiation.

The process of conduction involves the transfer of energy between materials through direct contact. Convection, on the other hand, involves the transfer of energy through the mixing of materials, which can occur through natural convection, where heat transfer results from the density difference between fluids, or through forced convection, where an external force such as a fan or compressor creates a pressure difference that facilitates mixing. Radiation is another form of heat transfer that occurs through the emission and absorption of energy via electromagnetic waves, such as visible or infrared light. The impact of heat transfer through radiation is negligible in the context of the heat pump system, but radiation plays an important role in heating buildings in direct sunlight [26].

In this project, the heat exchangers employed were of the closed-type variety, which are also known as recuperators. These devices use a wall or plate to physically separate the two fluid streams, facilitating both conductive and convective heat transfer to achieve the desired heat transfer effect. A common implementation of this design is the plate exchanger [27], which is the specific type utilized in the laboratory setting, as well as in

the Simulink model. The flow through the heat exchanger can be arranged in a variety of configurations, with the countercurrent flow configuration being the most energy-efficient option [28], which is also the configuration used in this project.

2.2 Heat Pump Cycle

Heat pumps are composed of four primary parts: a compressor, a condenser, an evaporator, and an expansion valve, illustrated in Figure 2.1. In this particular system utilizing CO_2 as the refrigerant, the fluid remains in a gaseous state and does not undergo condensation. Therefore, it is appropriate to refer to the condenser as a gas cooler.

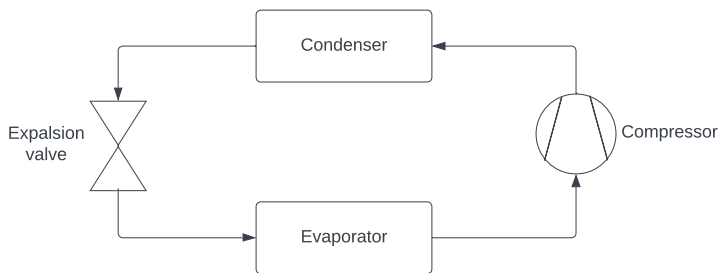


Figure 2.1: Schematic of a General Heat Pump System

The compressor raises the pressure and temperature of the refrigerant through an isentropic process, in which the entropy remains constant. The gas cooler, a plate heat exchanger, is used to heat the fluid that flows through the heating facility. The hot refrigerant gas enters the heat exchanger and heat is transferred from the gas to the fluid. The evaporator evaporates the fluid, resulting in a rise in both enthalpy and entropy. The expansion valve rapidly expands the refrigerant by reducing its pressure, causing a sudden drop in temperature through a throttling effect, where the valve achieves adiabatic expansion of the gas in the pipeline at a constant enthalpy.

Figure 2.2 illustrates the Pressure-Enthalpy Refrigeration Cycle for transcritical CO_2 heat pumps. The intermediate steps 1' and 3' in the figure represent the internal heat exchanger used in CO_2 heat pump cycles to superheat and sub-cool the fluid, which improves the coefficient of performance (COP) [29]. The internal heat exchanger is further explained in Section 2.2.1. The stages in the heat pump cycle are as follows: 1-1' represents the internal heat exchanger, 1'-2 represents the compressor, 2-3 represents the gas cooler, 3-3' represents the internal heat exchanger, 3-4 represents the expansion valve, and 4-1 represents the evaporator.

2.2.1 Transcritical CO_2 Heat Pump Cycle

The components of the CO_2 heat pump system include a compressor, gas cooler, expansion valve, evaporator, liquid separator, and internal heat exchanger. The compressor, gas

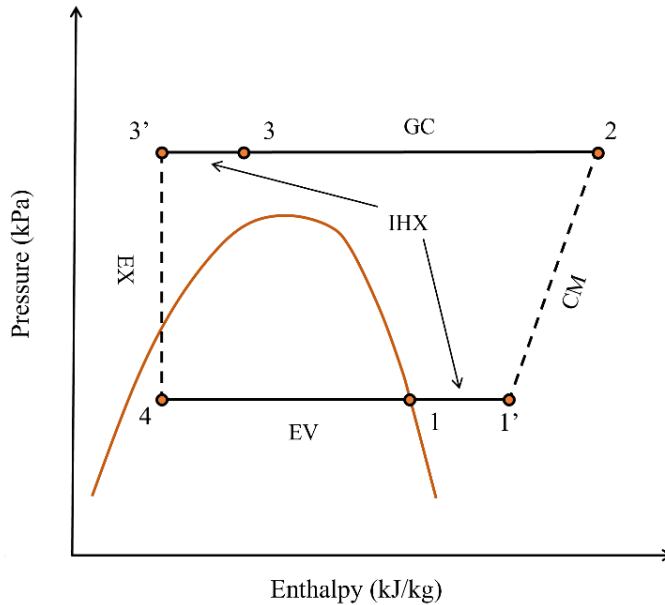


Figure 2.2: Pressure-Enthalpy diagram for trans-critical CO₂ heat pump. Figure from [30]

cooler, expansion valve, and evaporator are commonly found in all heat pump systems, as explained in the preceding paragraph. Figure 2.3 depicts a process diagram of the CO₂ heat pump cycle.

Incorporating an internal heat exchanger (IHX) is a common practice in CO₂ heat pump systems [31]. The primary objective of the IHX is to facilitate the transfer of heat from the high-pressure to the low-pressure side. By doing so, the hot, high-pressure CO₂ is sub-cooled before entering the expansion valve, while the cold vapor on the low-pressure side is superheated before entering the compressor. This heat transfer process results in a significant improvement in the system's overall performance and COP [29].

It is important to note that the physical system has a liquid separator which is used to separate out any liquids from the CO₂ vapor. Lubricants or other residual fluids that may have contaminated the stream must be removed before the refrigerant enters the compressor again. Given that the heat pump is installed indoors and thus not susceptible to frost buildup on the heat exchanger, the liquid separator has minimal impact on the system's performance. Its sole purpose is to ensure the proper functioning of the system, and the piece of equipment is therefore not included in the Simulink model.

The following paragraph describes the cycle that the CO₂ goes through, starting from the compressor. The compressor raises the pressure and temperature of CO₂, operating at a pressure of approximately 90 bar, representing the high-pressure side of the process. The refrigerant then passes through the gas cooler, which is a countercurrent heat exchanger that cools the refrigerant utilizing the water loop (the heat sink) that heats the facility. In the gas cooler, the refrigerant undergoes a transition from a vapor state to a denser

liquid-like gas state [32]. The liquid-like CO₂ gas is subsequently sub-cooled in the IHX and throttled by the expansion valve, which is regulated by a PI controller to maintain a constant discharge pressure. The valve induces a rapid pressure reduction, which causes a decrease in the fluid temperature, marking the low-pressure side of the system. The CO₂ enters the evaporator, where it undergoes evaporation at a constant temperature and absorbs heat. The glycol loop serves as the heat source, although its properties are beyond the scope of this discussion. Following the evaporation, any residual liquid is separated from the vapor in the liquid separator. Finally, the vapor is superheated in the IHX before re-entering the compressor and restarting the cycle.

2.3 Heating Facility

This section depicts and briefly describes the physical heating facility of the system. Connected to the heat pump is the heating facility that contains the heating devices. The facility is seen in Figure 2.4. There are five types of space heaters in the facility, including a large and a small fan coil, floor heating, and large and small radiators. Additionally, the heating facility includes a domestic hot water (DHW) tank, two control valves, and a pump. Although the physical system involves several components, the Simulink model introduced in the following chapter presents a simplified representation of the room. In the Simulink model, all five space heaters are combined into a single unit, and the DHW, control valves, and pump are not included.

Warm water is stored in the DHW tank and then leaves the tank and is regulated by a 3-way control valve (V1) to enter the heating facility. A pump (JP3) is used to transfer water into the space heaters. The flow of water into the floor heaters is regulated by another control valve (V2).

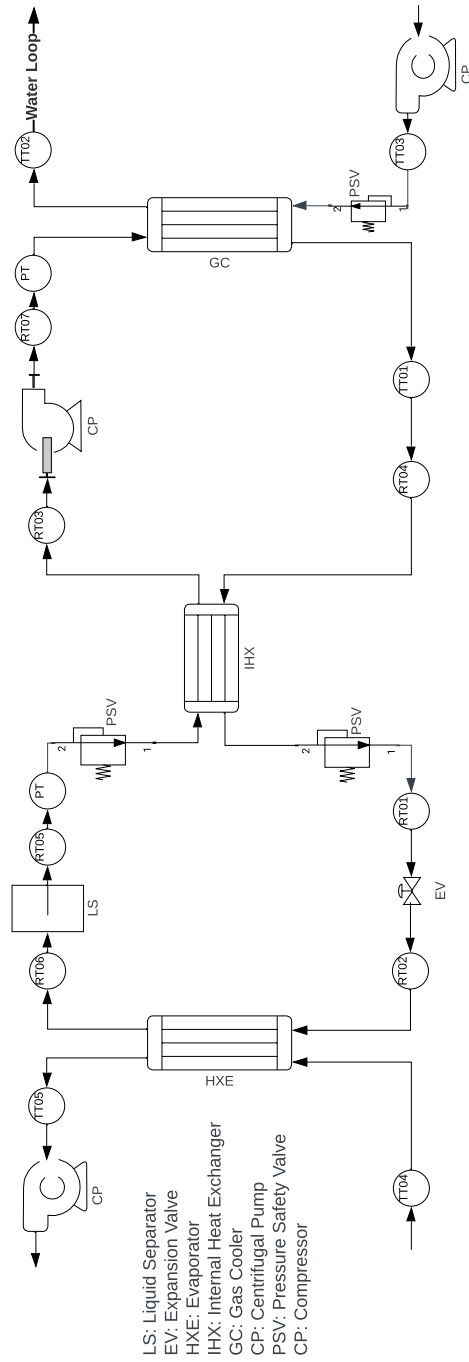


Figure 2.3: Process diagram of the heat pump cycle

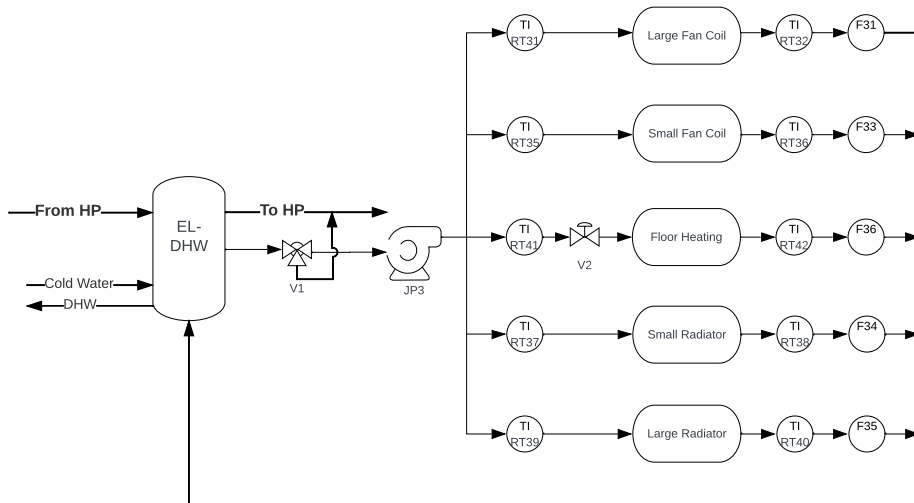


Figure 2.4: Process diagram of the heating facility

3

Modeling

Dynamic models are simplified representations of real-world processes and are used to describe the behavior of a system over time. The modeling of physical systems offers insights into how the system will respond to various inputs and operating conditions without having to conduct tests on the actual system. Investigating how a building responds to a step response in temperature may take hours or days, whereas simulating the step response using a model could take only a second or two. Lastly, advanced controllers need mathematical models to filter out disturbances or to predict future outputs. The MPC controller uses a model in addition to real data to predict future output values.

3.1 Modeling Paradigms

There are several types of models, and they are classified on how they are obtained [33]. In building modeling, three modeling paradigms are used - white-box, black-box, and gray-box modeling.

White-box

Theoretical models or white-box models are developed using physical equations such as the conservation laws for mass and energy. The parameters used in these models are physically meaningful and are obtained from the construction materials, the geometry of the building, and from equipment specifications. The major drawback of white-box modeling is that good models can become very complex and expensive to develop. Furthermore, some parameters in the model may be unavailable, such as heat transfer coefficients. In order to get an accurate model, thousands of parameters are often needed [16]. Since an accurate model relies on so many parameters, many potential sources of model inaccuracies are introduced. On the other hand, white-box modeling has the advantage of being easy to understand, and they are reliable over a wide range of conditions.

Black-box

Empirical models or black-box models are data-driven models obtained by fitting experimental data. The model describes the dynamics of the system solely based on data without having any prior knowledge about the physical states of the system. Black-box models are easy to develop but tend to only be accurate for the operating conditions used in the experimental data. Black-box models offer advantages over other model paradigms, such as lower development costs and the flexibility to use any signal as input or output, regardless of the underlying physics. However, these models have drawbacks, including the need for training data to create accurate models and their limited reliability beyond the range of the training data.

Gray-box

Gray-box modeling is a hybrid of the two above, where numerical values in the parameters are calculated using experimental data. This type of modeling includes a diverse range of models that incorporate simplified physical relationships and rely on parameter estimation using measured data. Typically, gray-box models simplify physics by reducing state-space dimensionality or linearizing the equations. Gray-box modeling is the most common type of model used in industrial processes [34], and is also the type used to model the heat pump system.

This type of modeling has the advantages of using physical equations, working well in a wider range of operating conditions, and they allow for parameter estimation. The gray-box approach addresses the limitations of both white-box and black-box models. Gray-box models, which already contain some knowledge about the system, tend to be more reliable outside the calibration range and require less data for calibration compared to black-box models. There is also a lower risk of overfitting. Gray-box models can be easily adapted to meet the requirements of MPC solvers by ensuring continuity, linearity, or differentiability. Additionally, gray-box models are portable between similar systems, and a few model types can represent the majority of buildings [35].

The selection of a specific paradigm is primarily influenced by the resources available, in addition to desired features of the model. Figure 3.1 shows a summary of the most common features for the three paradigms. For the purpose of modeling HVAC systems, where information about the building and HVAC system, in addition to some experimental data is available, the gray-box model approach is considered the most convenient [16]. A commonly used type of gray-box model used in thermal building modeling is the RC analogy, which establishes a connection between a model and an electrical circuit comprising resistors and capacitors, as discussed in the subsequent sections of this chapter.

3.2 Conservation Laws

In the physical realm, a conservation law is derived from a symmetry principle. There are numerous conservation laws, some of which are exact while others are only approximate [36]. Some conservation laws describe the flow of energy and mass, while others describe momentum and angular momentum. The most important conservation laws for this project are the conservation of mass and energy, and the laws of thermodynamics.

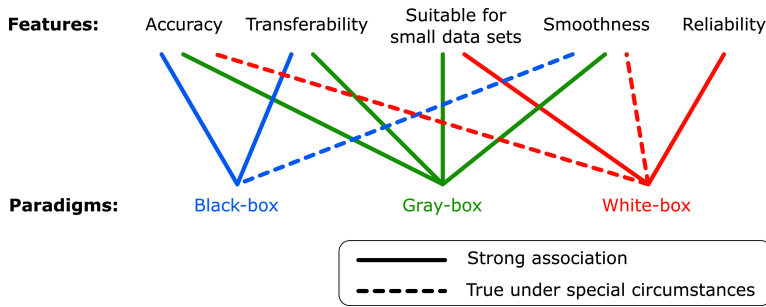


Figure 3.1: Overview of typical features of the three modeling paradigms. Figure from [16]

The law of conservation of mass states that mass is neither created nor destroyed, e.g. the total mass in a closed system will remain the same during chemical reactions or phase changes. The law of conservation of energy is very similar as it states that energy can neither be created nor destroyed - it can only convert from one form of energy to another.

The first law of thermodynamics states that energy cannot be created nor destroyed. As heat is a type of energy, a large focus when creating a room model is describing the flow of heat into and out of the room. The flow of energy in and out of the system ultimately determines the temperature of the room. The second law of thermodynamics states that energy passes from a warmer body to a colder body. Heating and cooling the room happens through heat transfer due to convection, conduction, and radiation, as described in Chapter 2. The laws of thermodynamics describe how heat is a form of energy that can be transferred from one place to another. Another form of energy that behaves similarly to heat is electricity. Both heat and electricity obey fundamental laws of physics and one can use this property as an analogy to better understand the behavior of thermal systems in terms of electrical concepts, and vice versa. This can be particularly useful in situations where it is easier to measure or manipulate electrical properties than thermal properties.

3.3 Thermal-electrical Analogy

Heat transfer through conduction is expressed with Fourier's law as:

$$q = \frac{\Delta T}{R_t} \quad (3.1)$$

Here, q represents the heat flow, ΔT represents the temperature difference, and R_t represents the conductive thermal resistance.

Ohm's law is another widely known equation that bears a striking resemblance to Eq. 3.1. By substituting q with current, I , and ΔT with voltage difference, ΔV , the equation gives Ohm's law. Ohm's law states that current flowing through a conductor is directly proportional to the change in voltage, and is expressed as:

$$I = \frac{\Delta V}{R_e} \quad (3.2)$$

Note that the subscript on the resistances in Eqs. 3.1 and 3.2 is utilized to differentiate between thermal resistance (R_t) and electrical resistance (R_e).

Both equations illustrate how energy is transferred through a substance by conduction. To establish the analogy between the two, the individual terms can be compared. In Fourier's law, q represents the heat flow or the rate of heat transfer through conduction, while I in Ohm's law denotes the flow of current. The temperature difference, ΔT , in Fourier's law measures the energy difference across a substance, whereas in Ohm's law, ΔV is the energy per unit charge. The resistance in Ohm's law explains a material's ability to impede the flow of electrical charge, while in Fourier's law, the resistance can be expressed as:

$$R_t = \frac{1}{UA} \quad (3.3)$$

Here, U represents the overall heat transfer coefficient and A is the area. In an electrical circuit, resistance limits the flow of current, while in a thermal system, resistance limits the flow of heat. Table 3.1 summarizes the main analogies between thermal and electrical systems, including their corresponding variables and parameters.

Thermal System	Electrical System
Temperature (T)	Electrical potential (voltage) (V)
Heat flow (q)	Electrical current (I)
Thermal resistance (R_t)	Electrical resistance (R_e)

Table 3.1: Thermal-Electrical Analogy

As seen from the paragraphs above, both Fourier's and Ohm's law describe a material's capacity to impede flow of energy through matter. When modeling the heat transfer in a room, using the thermal-electrical analogy makes modeling easier as it is simpler to measure or control electrical properties instead of thermal properties.

Due to the thermal-electrical analogy, the electrical library the Simscape extension in Simulink can be utilized to conveniently construct a room model by assembling resistors and capacitors. It is worth noting that the conventional modeling approach in Simulink using transfer functions could be employed instead of using the Simscape extension. However, this method requires Laplace transformations to be applied to each resistor and capacitor to obtain the transfer function. The adoption of standard components in Simulink for modeling is not only time-consuming but also leads to increased complexity and decreased comprehensibility of the model.

3.4 Modeling a Room

In the context of building thermodynamics, heat transfer occurs through three mechanisms: conduction, convection, and radiation. The predominant heat transfer modes within enclosed spaces are conduction via walls, floors, and ceilings, convection through radiators and air, and radiation via windows. Furthermore, the heat storage capacity of materials within the space also plays a role in altering the room temperature.

3.4.1 3R2C Model

A one-layer slab, such as a wall, is commonly modeled using a 3R2C model [9]. The 3R2C model, named after its three resistors and two capacitors, can be represented by an electrical circuit, as illustrated in Figure 3.2. Heat transfer via convection occurs between the outside temperature and the temperature at the outer wall surface, represented by the first resistor (R_{ow}). Within the wall, a capacitor represents heat storage, while the resistor represents conductive heat transfer. Two capacitors with identical values are required to obtain two differential equations for calculating the unknown temperatures at the inner and outer walls. Finally, the last resistor represents the convective heat transfer between the surface of the inner wall and the enclosed space. Using this model, the differential equations to determine the unknown temperatures, T_1 and T_2 , can be obtained as seen in Eqn. 3.4.

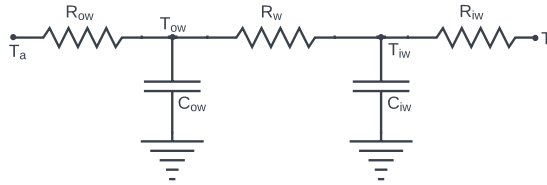


Figure 3.2: 3R2C model

$$\begin{aligned} C \frac{dT_{ow}}{dt} &= hA(T_a - T_{ow}) + \frac{T_{iw} - T_{ow}}{R} \\ C \frac{dT_{iw}}{dt} &= hA(T_r - T_{iw}) + \frac{T_{ow} - T_{iw}}{R} \end{aligned} \quad (3.4)$$

The one-layer slab RC model can be represented in state-space form as a discrete time-invariant system:

$$\mathbf{x}[k+1] = \mathbf{A}\mathbf{x}[k] + \mathbf{B}\mathbf{u}[k] \quad (3.5)$$

$$\mathbf{y}[k] = \mathbf{C}\mathbf{x}[k] + \mathbf{D}\mathbf{u}[k] \quad (3.6)$$

where \mathbf{x} is the state vector, \mathbf{y} is the output vector, \mathbf{u} is the input vector, and \mathbf{A} is the state matrix, \mathbf{B} is the input matrix, \mathbf{C} is the output matrix, and \mathbf{D} is the feedforward matrix.

The system in Figure 3.2 will have the state-space representation shown as:

$$\begin{bmatrix} \dot{T}_{ow} \\ \dot{T}_{iw} \\ \dot{T}_r \end{bmatrix} = \begin{bmatrix} -\frac{R_{ow}+R_w}{R_{ow}R_wC} & \frac{1}{R_wC} & 0 \\ \frac{1}{R_wC} & -\frac{R_w+R_{iw}}{R_wR_{iw}C} & \frac{1}{R_{iw}C} \\ 0 & \frac{1}{R_{iw}C} & -\frac{1}{R_{iw}C} \end{bmatrix} \begin{bmatrix} T_{ow} \\ T_{iw} \\ T_r \end{bmatrix} + \begin{bmatrix} \frac{1}{R_{ow}C} \\ 0 \\ 0 \end{bmatrix} [T_a] \quad (3.7)$$

3.4.2 Modeling the Walls and Ceiling

In terms of modeling, walls and ceilings can be considered equivalent as they both represent slabs in contact with an outer temperature and possess similar composition. The primary distinction between modeling a wall and a ceiling is the materials utilized, resulting in unique resistor and capacitor values. In the case of simulating a multi-story building, the outdoor temperature of the ceiling could be substituted with the temperature of the room located above. However, this particular scenario is not applicable to the current project. In fact, an assumption has been made that the walls and ceiling are constructed of identical materials, allowing them to be combined and represented as a single electrical component. This component can be represented similarly to the one depicted in Figure 3.2.

3.4.3 Modeling the Floor

The process of modeling the floor is comparable to modeling the walls and ceilings. If the room were located on an upper level, modeling the floor would be equivalent to modeling the ceiling. In this particular scenario, however, the floor comes into contact with the ground. It is assumed that the ground temperature is 0°C , and thus, an electrical ground is employed to simulate the ground's 0°C temperature. In Simscape, the electrical components employed to model the floor are depicted in Figure 3.3. The capacitor signifies the thermal mass, whereas the resistor represents the thermal resistance of the floor.



Figure 3.3: Model of the floor

3.4.4 Modeling the Window

In contrast to walls and floors, windows do not possess significant thermal mass, making it unnecessary to include a capacitor for thermal mass in the model. Instead, the heat transfer through the window is accounted for by considering the temperature difference between the inside and outside air. The electrical components utilized to model the window in Simscape are depicted in Figure 3.4.

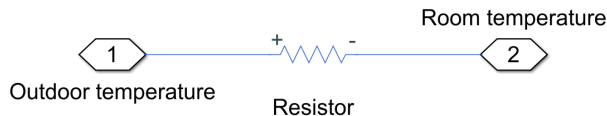


Figure 3.4: Model of the window

3.4.5 Room Model

A comprehensive model of the room can be created by interconnecting the building elements through Simscape components. Figure 3.5 illustrates the Simulink model of the room constructed using the Simscape electrical components. The values of the resistors and capacitors, as well as the connection port blocks for the outdoor temperature and radiator, both of which are defined as physical signals, are specified in a Matlab workspace.

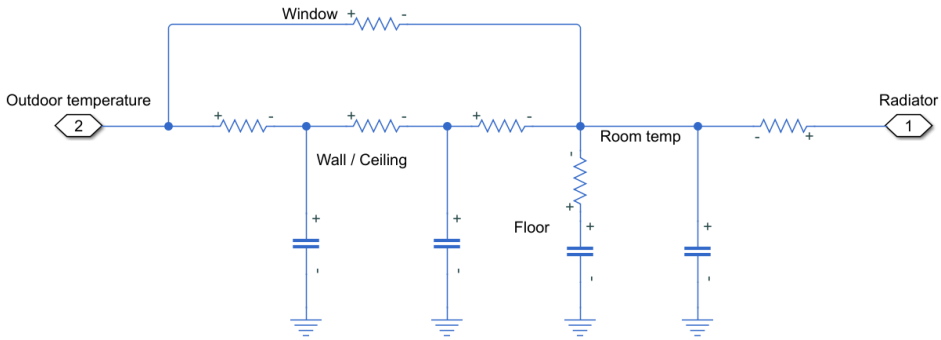


Figure 3.5: Simulink/Simscape model of the room

The current room model is relatively extensive as it includes heat loss through all surfaces. However, it does not take into account the heat loss from ventilation and infiltration, which can significantly affect the temperature development in a room by introducing heat or moisture from the outside. These factors were omitted from the model to prevent excessive complexity, but Section B in the Appendix provides information on how to incorporate ventilation and infiltration into the model.

The literature provides the heat transfer coefficients (h) for the building elements. Table 3.2 lists the convective heat transfer coefficients, which indicate how energy is transferred between a surface and a moving fluid. This energy transfer can occur due to forced convection, where a fluid is induced by an external force, or due to natural (or free) convection, which is caused by temperature differences in the fluid. Although the heating facility room modeled in this study is situated inside a building where forced convection occurs due to ventilation, the airflow of the external air is assumed to be small enough to be considered natural convection.

Type of Convection	h (W/(m ² · K))
Wall to air	3
Wall to window	5
Window to air	3
Radiator to wall	7

Table 3.2: Typical values of convective heat transfer coefficients in buildings. Values found in [37]

The overall heat transfer coefficients (U) indicate how well heat is conducted through

resistant mediums. A higher coefficient indicates that heat can be transferred more easily between the medium. Building elements, typically consisting of multiple layers of materials have distinct heat transfer coefficients for each layer. However, in this project, an approximation is made where each building element is assigned a single coefficient. The overall heat transfer coefficients used in the model are defined in Table 3.3.

Building Element	U (W/(m² · K))
Exterior wall	0.3
Interior wall	0.9
Window	2.3
Floor	3.0
Ceiling	2.2

Table 3.3: Typical values of overall heat transfer coefficients in building elements. Values found in [38]

3.5 Verification of the Room Model

To verify the accuracy of the room model, simulations were conducted to ensure that the temperature evolution matched the expected behavior.

A simulation of the room was performed to validate the one-layer slab used to model heat transfer through the wall. No external heat was introduced to the room, so the temperature development was driven solely by the initial temperature differences between the indoor and outdoor air. Figure 3.6 depicts the temperature changes in the room over a 24-hour period. The initial indoor temperature was set to 20°C, the initial wall temperature was set to 10°C, and the outdoor air temperature was set to 5°C. The simulation results demonstrate that the temperature of the room approaches that of the outdoor temperature. As no heat is added to the room, and the surrounding temperature is lower, it is expected that the room temperature will converge to the ambient temperature, in accordance with the second law of thermodynamics, which states that energy flows from hotter objects to colder ones.

In order to expand the scope of the testing, the model was subjected to varying outdoor temperatures. Figure 3.7 illustrates the response of the system to outdoor temperatures that fluctuate throughout the day. To represent the daily temperature fluctuations, an input signal consisting of a sine wave with an amplitude of 2, a bias of 5, and a frequency of 0.0002 rad/sec was added as an input. The results indicate that the room temperature initially drops towards the outdoor temperature and then begins to follow the same oscillation pattern, although with a slight time delay. This delay is a result of the substantial thermal mass present in the building components. Due to the walls' ability to store heat, the process of dissipating and absorbing heat from the external environment is a sluggish one, which is also why the room temperature never reaches the extremes of the outdoor temperature.

The two plots indicate that the temperature progression in the room is behaving in a predictable manner. As a result, the model effectively mirrors the physical system and will

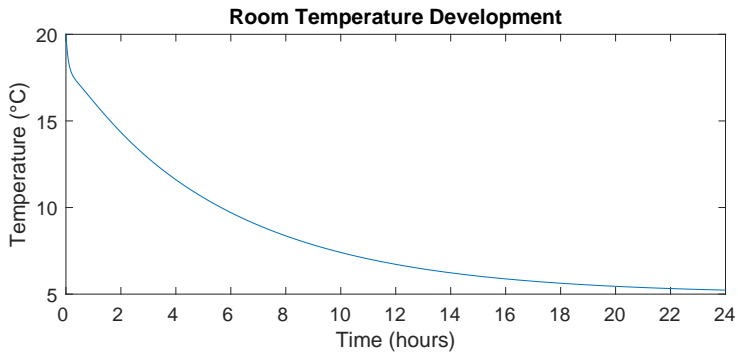


Figure 3.6: Room temperature development over 24 hours, with outdoor temperature at 5°C, initial wall temperature at 10°C, and initial indoor temperature at 20°C.

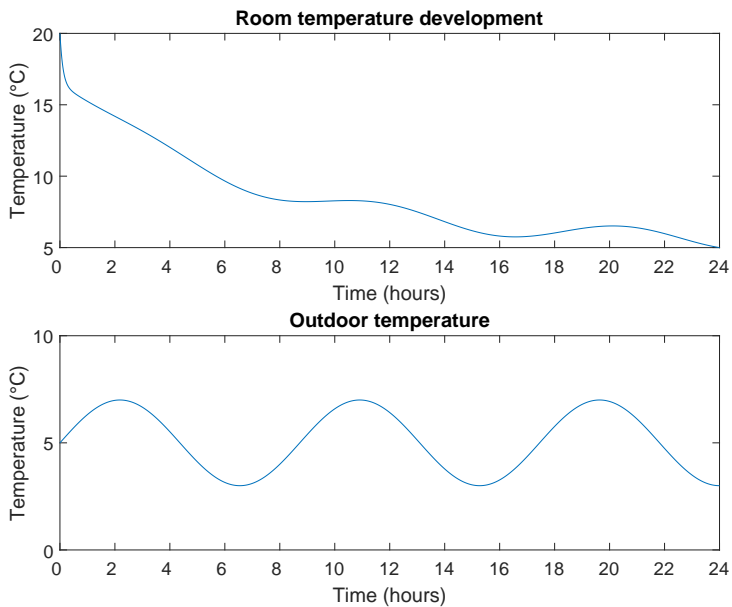


Figure 3.7: Room temperature development over 24 hours, with the outdoor temperature fluctuating between 2 and 7°C, initial wall temperature at 10°C, and initial indoor temperature at 20°C.

be utilized as a simplification of the physical system to incorporate controllers into the model and analyze them comparatively.

3.6 Modeling the CO₂ Cycle

In this section, a model of the CO₂ heat pump cycle is developed and implemented in Matlab/Simulink. A description of the CO₂ heat pump cycle was presented in Chapter 2. Simulating this CO₂ cycle, especially during the high-pressure phase in the supercritical fluid region, is a challenging task to develop from scratch in Simulink. However, MathWorks provides an example model of a transcritical CO₂ refrigeration cycle, which can be accessed by executing the command `ssc_transcritical_refrigeration` in a Matlab command window. While the MathWorks example model is designed for refrigeration cycles, it can be used in heating cycles since the two cycles are fundamentally identical, differing only in their usage. The refrigeration cycle cools the external fluid flowing through the evaporator, while the heat pump cycle heats the external fluid flowing through the condenser. The MathWorks model has been adapted and implemented in this project, as shown in Figure 3.8, and is explained in the following paragraphs.

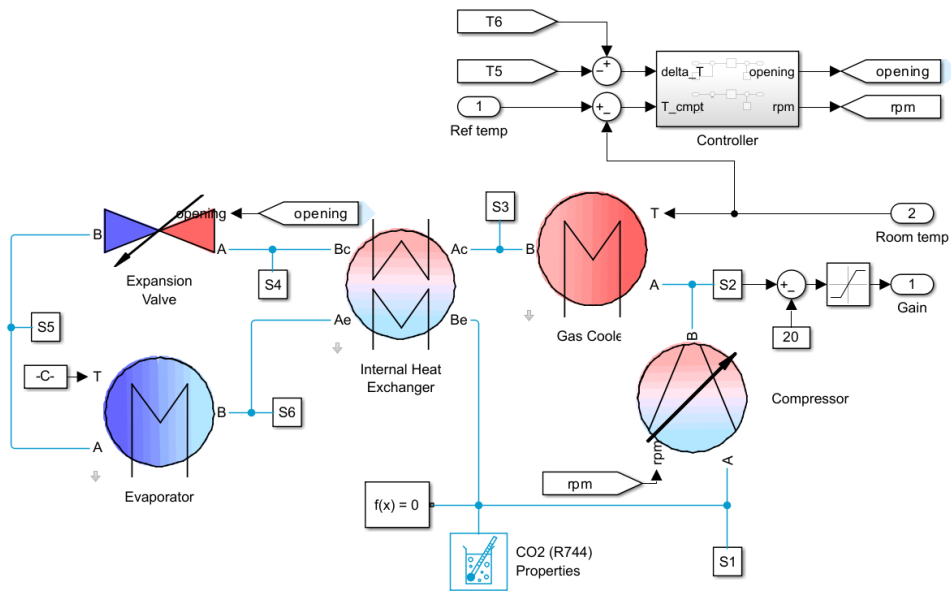


Figure 3.8: Simulink model of transcritical CO₂ heat pump cycle

Figure 3.8 employs various Simscape Foundation libraries, including Two-Phase Fluid Models, Thermal Models, and standard Simulink models. The Two-Phase Fluid library is utilized because the working fluid comprises a mixture of liquid and gas components. The library incorporates a Two-Phase Fluid Properties (2P) block, which specifies the properties of the CO₂. The Thermal Models are used to model fundamental thermal effects like insulation and heat exchange.

To ensure proper regulation of the CO₂ cycle, two controllers are employed—one for the expansion valve opening and another for the compressor speed. When the two-phase CO₂ mixture enters the evaporator, the temperature at the evaporator’s inlet, T5, aligns

with the saturation temperature. Therefore, the difference between T6 and T5 represents the extent of superheat within the evaporator, which is controlled through the adjustment of the expansion valve. Meanwhile, the room temperature is governed by a controller that modulates the shaft speed to achieve the desired flow rate. In the MathWorks example model, PID control is utilized to regulate both the expansion valve and the compressor. While the controller remains the same in the modified version, different values for K_p and K_i have been determined to enhance performance. Later in the project, the PID controller on the compressor is replaced with an MPC to allow for a comparison between the two control types.

The heat exchange between the radiator and the hot CO₂ stream, which enters the gas cooler, is simplified as a constant delta T of 20 °C, also known as the minimum approach temperature. The minimum approach temperature is the smallest temperature difference between the hot and cold streams. In an ideal, infinitely large heat exchanger, where all the heat from the hot stream was transferred to the cold stream, the temperature difference would be 0°C. In practice, however, some heat is lost in the process. Factors such as the design of the heat exchanger, flow rates, and thermodynamic properties of the fluids affect the minimum approach temperature. Typical values for the minimum approach temperature falls within the range of 5°C to 30°C [39], hence 20 °C is selected for the heat exchanger used in the gas cooler.

4

Automatic Control

All automatic controllers have the purpose of adjusting the inputs to a system in order to attain a desired setpoint or trajectory, without human interaction. By implementing automatic controllers in industrial processes, one can regulate the behavior of complex systems, while ensuring safe and efficient operations. There are several types of automatic controllers, and the choice of control is often dependent on the type of system to be controlled. In general, the more complex and precise the control task, the more sophisticated the controller needs to be. Two common controllers are the PID controllers, which are widely used in industrial processes, and the MPC, which are popular in advanced control applications [33].

The PID controller is a control technique that measures the error between a desired setpoint and the actual output of the system, and then uses the three terms (proportional, integral, and derivative) to calculate a gain in order to minimize the error. The MPC controller, on the other hand, is an advanced control technique that uses a model of the system to predict future behaviors and calculates an optimal input based on the model and on the current output of the system. MPC minimizes a cost function over a finite time horizon that is subject to constraints on the inputs, outputs, and states of the system. The main difference between the two control techniques is that PID uses the current error to calculate a new gain, while MPC uses a model in addition to the current error to predict how the system will behave in the future and calculates the gain accordingly. Implementing MPC is more complex, but is effective for controlling nonlinear, complex dynamics, or systems subject to constraints. The PID controller is simpler and is usually sufficient for controlling linear systems with simple dynamics.

Both control techniques have been implemented in this project to investigate how much more efficient, if any, the advanced MPC scheme is able to regulate the room temperature compared to the PID. This chapter presents the theoretical foundations of the two controllers. Some of the theory behind the PID controller is based on the theory presented in the specialization project [25].

4.1 PID Control

In the realm of process control, the PID controller is widely employed [33], comprising of proportional, integral, and derivative control modes. As previously mentioned, the fundamental purpose of feedback control is to minimize the error signal $e(t)$. The error is expressed as:

$$e(t) = y_{sp}(t) - y_m(t) \quad (4.1)$$

where y_{sp} is the set point, and y_m is the measured controlled variable. The proportional control mode involves multiplying a constant K_c with the error signal to compute the gain. The integral control mode calculates the gain from the integral of the error signal over time. When a deviation from the set point is detected, the integral action accumulates the recent error and adjusts the gain to eliminate the offset. The derivative control mode uses the rate of change of the error signal to determine the gain.

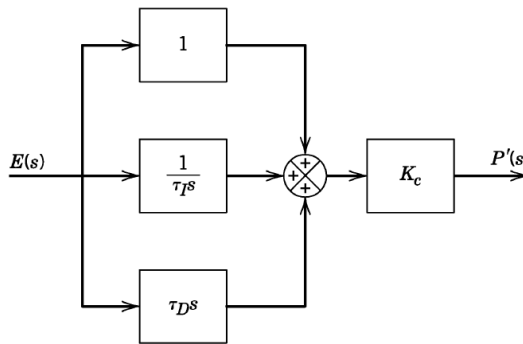


Figure 4.1: Block diagram of parallel PID controller. Figure from [33]

There exist various types of PID controllers, but the parallel form is used and implemented in Matlab and is seen in Figure 4.1. The corresponding control equation is expressed as:

$$p(t) = \bar{p} + K_c \left(e(t) + \frac{1}{\tau_I} \int_0^t e(t^*) dt^* + \tau_D \frac{de(t)}{dt} \right) \quad (4.2)$$

where \bar{p} denotes the steady-state bias, τ_I represents the integral or reset time, and τ_D represents the derivative time. The application of Laplace transformation yields the transfer function expressed as:

$$\frac{P'(s)}{E(s)} = K_c \left(1 + \frac{1}{\tau_I s} + \tau_D s \right) \quad (4.3)$$

In numerous processes, incorporating the derivative control mode with a non-zero value can improve the dynamic response to the controlled variable. The derivative term, when coupled with integral action, typically offsets the destabilizing influence of the integral effect. However, when dealing with noisy processes, utilization of the derivative

action can intensify the noise. Installing a low-pass filter can reduce the noise, but in most processes, a PI controller proves to be satisfactory [33].

The PID controller presented in Eq. 4.3 is an ideal controller and disregards the physical constraints imposed on the system. For instance, the heat pump system is subject to physical limits on the valve opening and the heat exchangers, each having an upper and lower value. Newton's Law of Cooling governs the rate of heat transfer between the hot and cold streams, which depends on the temperature difference. The hot stream cannot exit the heat exchanger at a temperature lower than the cold stream's entering temperature. When the controller output exceeds its physical constraints, the controller becomes saturated. Using a controller output gain beyond the system's physical limits generates a persistent error, which causes the integral term to grow progressively over time. The additional accumulation of the integral after the controller is saturated is termed integral or saturation windup. The integral term keeps increasing until $e(t^*) \neq 0$, and only decreases when the error changes its sign. The PID Controller block in Simulink has built-in options for handling saturation limits and anti-windup mechanisms.

4.1.1 Tuning Methods

Tuning controllers have a major impact on the closed-loop stability of the system. Various techniques can be employed to adjust PID controllers, including transient response, frequency response, and the utilization of transfer function models. Ziegler-Nichols (Z-N) and Skogestad's Simple Internal Model Control (SIMC) are two widely used analytical methods for tuning controllers. The trial and error method is also a feasible tuning strategy. The Z-N and SIMC methods are briefly described in this section, but a more in-depth description can be found in Section C in the Appendix.

A well-tuned PID controller satisfies a few performance criteria. Most importantly, the closed-loop system must be stable. Furthermore, effects from disturbances should be minimized, the set-point changes are smooth and quick, the steady-state error should be eliminated, and the control system should be robust. Tuning controllers involves a trade-off between performance and robustness. It is desired that the controller can handle disturbances and setpoint tracking while also being able to operate in a wide range of conditions. The controller should therefore be a balance between the two.

Ziegler-Nichols Method

The Ziegler-Nichols tuning method is a popular heuristic method for tuning PID controllers. It involves applying step responses to obtain a process reaction curve, from which the ultimate gain and period are determined. These values are then used to find the controller parameters. The method is relatively simple to use and has been widely adopted, but can result in oscillations or overshoot in the response [33].

SIMC Method

Simple Internal Model Control is a tuning method used for processes with significant dead-time [33]. In SIMC, a simple model is used to estimate the dead-time of the process, and the controller parameters are adjusted accordingly. The method can provide a good

balance between stability and performance, and it has been shown to work well in practice for many processes with time delay [40].

Typical Responses of Feedback Control Systems

Instead of using analytical tuning methods such as the Z-N and SIMC methods, trial and error can also be utilized to tune PID controllers. This approach involves adjusting the controller parameters based on the operator's experience and judgment, rather than relying on mathematical or analytical methods. This paragraph aims to briefly summarize the qualitative impact of modifying individual controller parameters. In general, increasing the controller gains leads to a more aggressive system response, but only up to a certain point. Setting K_c too high can cause excessive oscillations or instability. Raising the integral time, τ_I , usually slows down the controllers. It is more complicated to generalize the effect of changing τ_D , but increasing it when the gain is small typically results in reduced overshoot, settling time, and oscillations. However, if τ_D is too large, measurement noise is amplified, which can lead to unwanted oscillations. Table 4.1 provides a summary of the effects of increasing the individual controller parameters. For more detailed information on increasing the controller parameters, see [33].

	Rise time	Overshoot	Settling time	Steady state error
K_p	Decrease	Increase	Small change	Decrease
K_i	Decrease	Increase	Increase	Eliminate
K_d	Small change	Decrease	Decrease	Small change

Table 4.1: Effect of increasing the individual controller parameters.

4.2 Model Predictive Control

When controlling multiple-input multiple-output processes with constraints, model predictive control is a commonly used control technique [33]. By having a dynamic model of the process, in addition to using current measurements, the control scheme is able to predict future output values. From this calculation, the input variables are calculated based on the predictions from the model and the current measurements. The output variables are often referred to as the controlled variables or CVs, and the input variables are referred to as the manipulated variables or MVs. The disturbance is the difference between the prediction and the measured variables and is called disturbance variables or DVs.

MPC is often used in addition to the standard PID controller as it has a few additional advantages. The main objective for the MPC controller is summarized as follows by Qin and Badgwell [41]:

- Prevents violations of constraints on inputs and outputs.
- Adjusts some output variables to their optimum, while others are maintained within specified ranges.
- Limits excessive changes in input variables.
- Is able to control process variables even when sensors or actuators are not available.

A block diagram of the MPC control scheme is shown in Figure 4.2. A process model is used to predict the output variables. The difference between the process output and the model output is used as feedback to the prediction block. The predicted outputs are used for setpoint calculations and control calculations. A cost function is used as an optimization objective to find the setpoints for the control calculations.

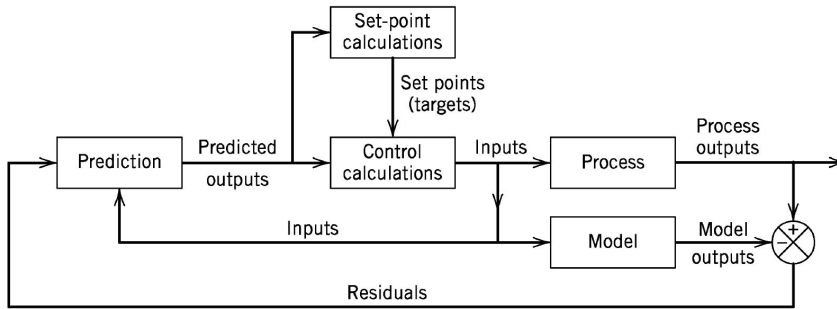


Figure 4.2: Block diagram of the MPC control scheme. Figure from [33]

The calculations done by the controller are based on current measurements and predicted future outputs. The MPC control calculations then determine a sequence of future control actions. Figure 4.3 shows how the actual output, y , predicted output, \hat{y} , and the manipulated input, u , change through the sampling time. At the current sampling time, k , a set of M values of the input are calculated. Both the current input $u(k)$ and the future inputs $M - 1$ are included in the set. This set of M values is the number of control moves, also called the control horizon. After M control moves, the input is held constant. The MPC calculates the inputs so that a set of P predicted outputs (with P being the prediction horizon) reaches the setpoint as effectively as possible. Based on this prediction, the controller computes an optimal control sequence that minimizes a given cost function over the time horizon. The optimal control sequence is then applied to the system only for the first step of the predicted time horizon. After this first step, the system's actual behavior is measured and fed back to the controller, which updates its prediction for the remaining time horizon and repeats the process.

4.2.1 MPC Toolbox in Matlab

The Model Predictive Control toolbox in Matlab is a powerful product that provides functions, an app, and Simulink blocks for developing the controller. The toolbox supports both linear and nonlinear problems, where implicit, explicit, adaptive, and gain-scheduled MPC's can be designed for linear problems, and single- and multi-stage nonlinear MPC's can be designed for nonlinear problems [42]. The performance of the controller can be evaluated by running closed-loop simulations in Simulink. For linear MPC, where the plant and constraints are linear and the cost function is quadratic, the standard MPC block in Simulink can be used to design a controller.

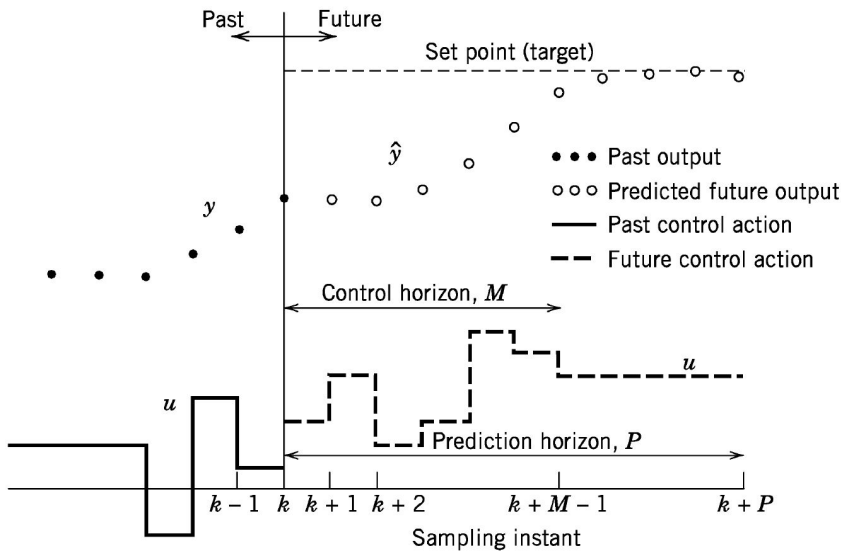


Figure 4.3: General concept of the MPC control scheme. Figure from [33]

Design Workflow

This paragraph provides a brief overview of the steps involved in the MPC design process. A comprehensive guide can be found in the Documentation for the Model Predictive Control Toolbox [42]. First, the internal plant model is defined by linearizing a nonlinear plant or identifying it using System Identification Toolbox software. The plant signals are then categorized into different input and output types. An MPC object is created in the MATLAB workspace or in the MPC designer, specifying controller parameters such as the sample time, prediction and control horizons, cost function weights, constraints, and disturbance models. Now that the controller has been created, the performance of the controller is evaluated by simulating the closed-loop response. Tuning the controller parameters can be done in the MPC Designer. Refining the closed-loop design may be necessary and is done by adjusting controller parameters and evaluating simulation scenarios. Other considerations include using manipulated variable blocking, setting reference targets for over-actuated systems, tuning Kalman state estimator gains or designing a custom estimator, and specifying terminal constraints. Before the MPC is deployed, the design is often optimized for future simulations, and to reduce the computational cost. This can be done by increasing sample time, shortening prediction and control horizons, limiting the maximum number of iterations in the optimization problem, and by tuning the solver. The controller may now be deployed to Matlab and Simulink.

Prediction Models

MPC uses plant, disturbance, and noise models for prediction and state estimation [42]. Figure 4.4 illustrates how the plant, disturbance, and noise models appear in the controller.

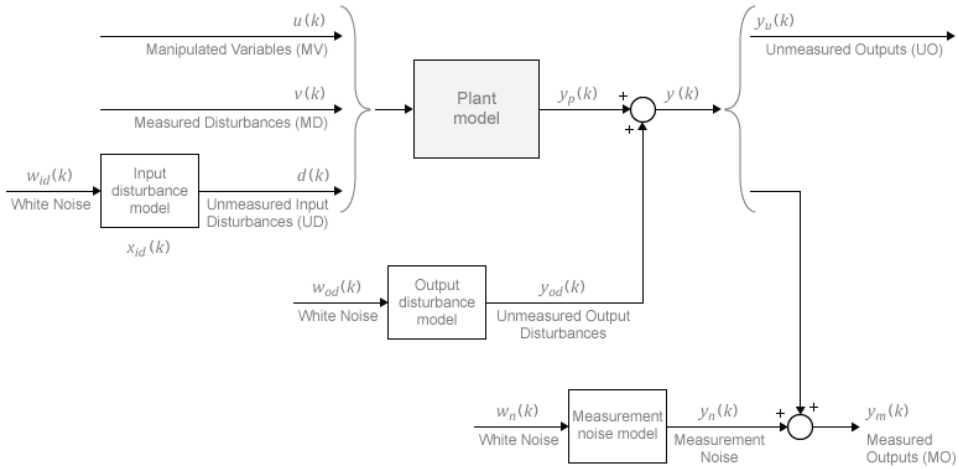


Figure 4.4: Model structure used in an MPC controller. Figure from [42]

The plant model must be on a linear-time-invariant (LTI) format, and can be specified using numeric methods like transfer functions or state-space representation, or identified using system identification. All estimations and optimizations in the MPC are done using discrete-time, delay-free, state-space systems with dimensionless input and output variables [42]. The MPC software performs the required computations to get the plant model on the correct form:

$$x_p(k+1) = A_p x_p(k) + B_{pu} u(k) + B_{pv} v(k) + B_{pd} d(k) \quad (4.4)$$

$$y_p(k) = C_p x_p(k) + D_{pu} u(k) + D_{pv} v(k) + D_{pd} d(k) \quad (4.5)$$

where $C_p = S_o^{-1} C$, B_{pu} , B_{pv} , B_{pd} are the columns of BS_i . D_{pu} , D_{pv} , D_{pd} are the columns of $S_o^{-1} DS_i$, and $u(k)$, $v(k)$, $d(k)$ are the manipulated variables, measured disturbances, and unmeasured input disturbances, respectively [42].

The plant model may include unmeasured input disturbances. The input disturbance model can be provided as a state-space, a transfer function, or as a zero-pole-gain object, and the MPC controller converts the model to the required form. If no input disturbance model is provided, a default model is used (see the Getting Started Guide for details [42]). An output disturbance model may also be provided. This type of model is often used in practice since the output is added directly to the plant, instead of affecting the plant states as the input disturbance does. If no output disturbance model is specified, a default model is used. The measurement noise model is used to help the controller distinguish between disturbances and measurement noise by specifying the noise type and its characteristics. The noise model can be provided to the controller, if not provided, a unity static gain is used.

Cost Function

The MPC solves a quadratic program (QP) optimization problem at each control interval. The optimization problem includes a cost function that penalizes deviations of the predicted inputs from the reference trajectory. Having high deviations is undesired, so the controller aims to minimize the function. The cost function is a scalar, non-negative measure of the controllers' performance, and for output reference tracking is formulated as:

$$J_y(z_k) = \sum_{j=1}^{n_y} \sum_{i=1}^p \left\{ \frac{w_{i,j}^u}{s_j^u} [r_j(k+i|k) - y_j(k+i|k)] \right\}^2 \quad (4.6)$$

where k is the current control interval, p is the prediction horizon, n_u is the number of manipulated variables, z_k is the QP decision given by:

$$z_k^T = [u(k|k)^T \quad u(k+1|k)^T \quad \dots \quad u(k+p-1|k)^T \quad \epsilon_k] \quad (4.7)$$

$y_j(k+i|k)$ is the predicted value of the j th plant output at the i th horizon step, $r_j(k+i|k)$ is the reference value for the j th plant output at the i th horizon step, s_j^y is the scale factor for the j th plant output, and $w_{i,j}^y$ is the tuning weight for the j th plant output at the i th horizon step. n_y , p , s_j^y , and $w_{i,j}^y$ are constants defined by the controller specifications.

The controller receives reference values, $r_j(k+i|k)$, over the prediction horizon. The controller then uses a state observer to predict the plant outputs, $y_j(k+i|k)$, based on the current state estimates, z_k , and the measured disturbances. The state observer is a mathematical model that estimates the current state of the plant based on the available measurements. Since the controller state estimates and MD values are available at interval k , the controller can use this information to update its predictions of the plant outputs and adjust the manipulated variables, z_k , to bring the actual plant outputs closer to the desired setpoints. See [42] for more details about the MPC Toolbox in Matlab.

5

Controller Implementation

This project involves the implementation of two control strategies: the widely used PID and the more sophisticated MPC control strategy. To test the controllers, two models are used in the simulations. The first model involves a simplified radiator, whereby the controller regulates the radiator gain output to heat up the room. The second model comprises the transcritical CO₂ cycle, and the controllers regulate the expansion valve opening and compressor speed to adjust the room temperature.

In the first model, the controlled variable is the room temperature, and the manipulated variable is the radiator gain, which is adjusted to achieve the desired setpoint temperature. In the second model, when the transcritical CO₂ cycle is integrated, the manipulated variables become the expansion valve opening and compressor speed. The outdoor temperature, on the other hand, serves as a disturbance to the system and is thus referred to as the disturbance variable. An overview of the controlled, manipulated, and disturbance variables are listed in Table 5.1.

Controlled variables (CV)	Manipulated variables (MV)	Disturbance variables (DV)
Room temperature	Radiator gain Expansion valve opening Compressor speed	Outdoor temperature

Table 5.1: Controlled, manipulated, and disturbance variables in the system.

5.1 Implementation for the Simplified Radiator

5.1.1 Implementation of PID in Simulink

Adjusting the temperature in the room using PID control is done by sending a signal from the controller to an actuator to regulate the temperature in the radiator. The controller uses feedback to find the error between the desired setpoint and the measured temperature and

calculates an output based on the error. The PID controller block in Simulink is used in the simplified radiator model can be seen in Figure 5.1.

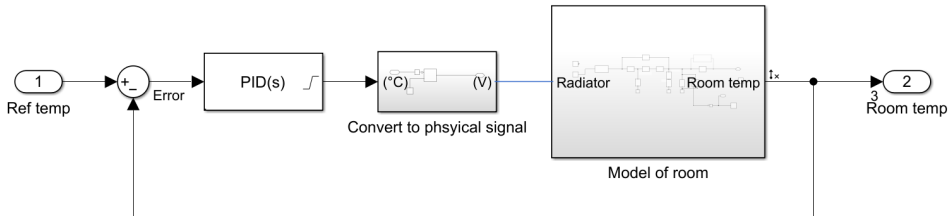


Figure 5.1: Simulink model of room with PID control to regulate the temperature of the radiator

Achieving fast set point tracking with minimal oscillations is a key requirement for a well-tuned PID controller. Several analytical methods for tuning PID controllers are available, including transfer function models, transient response, and frequency response, as discussed in Section 4.1.1. The trial and error approach was employed in this project to determine the optimal control parameters.

The optimal PID parameter values were identified as follows:

$$K_p = 40$$

$$K_i = 0.1$$

$$K_d = 0$$

Here, the radiator gain is the manipulated variable, whereas the room temperature is the controlled variable.

5.1.2 Implementation of MPC in Simulink

Implementing MPC in a Simulink model involves several steps. First, a simulation is designed that encompasses both the plant model and the MPC controller. The inputs and outputs of the controller are defined, and the controller block in Simulink is configured accordingly. The simulation is then executed to assess the performance of the control system.

The implementation of the MPC controller used in the simplified radiator model is seen in Figure 5.2. The plant model, which represents the room model in this case, is defined within the 'Model of room' block. The MPC controller is designed within the MPC block. Within this block, the prediction model, cost function, and constraints are specified. The prediction model is employed to forecast the future behavior of the system, while the cost function optimizes the control action. Constraints ensure that the control action adheres to certain limits or requirements.

The MPC block takes the plant model and the MPC controller as inputs and generates the control action as an output. Parameters such as sampling time, prediction horizon, and control horizon are specified. To form a closed-loop system, the MPC block is connected to the plant model. By doing so, the MPC controller can generate the control action

based on the predicted behavior of the plant model. Finally, the performance of the MPC controller is evaluated by analyzing the closed-loop response of the system.

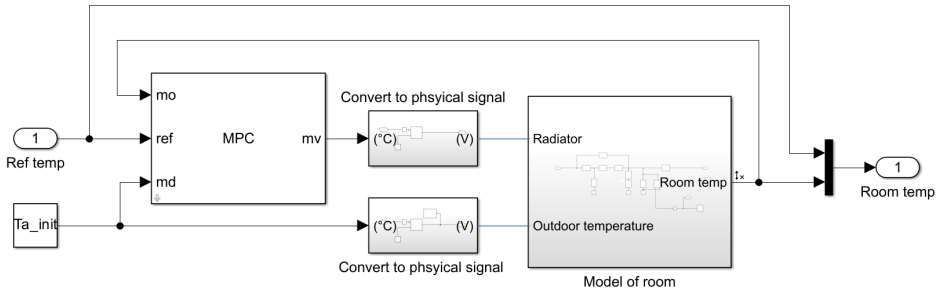


Figure 5.2: Simulink model of the room with MPC

The MPC controller is created using the linearized plant as an internal prediction model. The linearized plant model is written as a continuous-time state-space model, with the following A , B , C and D matrices:

$$\begin{aligned}\mathbf{x}(t+1) &= \mathbf{A}\mathbf{x}(t) + \mathbf{B}\mathbf{u}(t) \\ \mathbf{y}(t) &= \mathbf{C}\mathbf{x}(t) + \mathbf{D}\mathbf{u}(t)\end{aligned}$$

where

$$\mathbf{A} = \begin{bmatrix} -0.0004104 & 4.737e-09 & 0.0001754 & 0 \\ 1.992e-08 & -0.003324 & 0.0009881 & 0.001605 \\ 0.0001754 & 0.000235 & -0.0004104 & 0 \\ 0 & 0.0001718 & 0 & -0.0001718 \end{bmatrix},$$

$$\mathbf{B} = \begin{bmatrix} 0 \\ 0.000244 \\ 0 \\ 0 \end{bmatrix}, \quad \mathbf{C} = [0 \quad 1 \quad 0 \quad 0], \quad \mathbf{D} = 0$$

It should be emphasized that the matrices labeled A , B , C , and D are unique for the specific Simulink model used. For instance, the matrices used in the internal prediction model when the CO_2 cycle is included in the model (see Section 5.2) will be different.

Scale Factors

Specifying the scale factors of the input and output variables in the plant is important when the variables are of different magnitudes. Implementing scaling factors provides multiple advantages, including optimizing default MPC tuning weights for signals of similar magnitudes, simplifying the selection of cost function weights based on relative priorities, and enhancing numerical conditioning by mitigating the influence of round-off errors in calculations. The scale factor should reflect the span of the variable, which is defined as the difference between its maximum and minimum values in the units of measurement used

in the plant model. Internally, the MPC divides each plant input and output signal by its respective scale factor, resulting in dimensionless signals. See the Matlab MPC Documentation [42] for more details.

There are two plant input variables - the manipulated variable, MV, and the measured disturbance, MD. There is one plant output which is the measured output, MO. The input and output variables for the MPC used in the simplified radiator model have the following scale factors:

MV: 50
MD: 1
MO: 4

Tuning Weights

A good MPC controller usually requires some tuning of the weights in the cost function. To achieve a unique solution for the QP problem used in the controller, it is essential to select appropriate cost function parameters (penalty weights) and horizons that ensure the QP's Hessian matrix is positive-definite. Increasing the penalty weight on the manipulated variables ensures a positive-definite Hessian, but may result in a slower controller response [42]. The penalty weights assigned to the output variables (OV) also alter the Hessian matrix. Non-zero OV values prioritize OV target tracking and also increase the likelihood of a unique QP solution.

The penalty weights used in the MPC when using the simulation of the simplified radiator are:

MV: 0.1
MO: 2

Sample Time and Horizons

The choice of sample time, prediction horizon, and control horizon for the MPC controller depends on the requirements of the application and the dynamics of the system. Some of the factors to be taken into account include:

1. System dynamics: It is desired to have a sample time small enough to capture the important dynamics of the system. However, having a too short prediction horizon may not provide enough information for the controller to accurately predict the behavior of the system, while a too large horizon may cause poor controller performance.
2. Control objective: The prediction and control horizons should be chosen based on the control objective. For systems where the objective of the controller is to maintain the temperature of a room within a narrow range, the prediction horizon should be shorter, allowing for the controller to respond quickly to changes in temperature.
3. Computational resources: Higher prediction and control horizons require more computational power, which may be a challenge in real-life control applications. These parameters should therefore be chosen with consideration for what computational resources are available.

4. Actuator constraints: Upper and lower limits on the actuator should also be considered when choosing the prediction and control horizons. E.g. there may be maximum and minimum values on the control input. A control horizon that is too high may generate control inputs outside these limits.
5. Measurement noise: Measurement noise can affect the accuracy of the controller measurements. A shorter sample time may be needed when high amounts of measurement noise is present.
6. Disturbances: The choice of prediction and control horizon also depend on the amount and impact of disturbances on the system. For systems with frequent disturbances, a long prediction horizon may be desirable for the controller to account for the disturbances.

Based on the factors listed above, the sample time, prediction horizon, and control horizon for the MPC controller were chosen to be:

Sample time: 30
Prediction horizon: 10
Control horizon: 2

Constraints

Adding constraints to the controller is essential to ensure that the system operates within its physical limits. Constraints enable the controller to make informed decisions and generate control actions that balance performance and feasibility. An upper limit of 100°C was set as the constraint on the manipulated input variable.

5.2 Implementation for the CO₂ Cycle

Figure 5.3 shows how the room model is connected to the transcritical CO₂ heat pump cycle. The CO₂ Heat Pump system block, introduced in Chapter 3 and shown in Figure 3.8, is connected to the 'Model of room' block through the radiator gain. The controller in the 'CO₂ Heat Pump' block receives feedback of the room temperature and the desired setpoint temperature to regulate the shaft speed.

5.2.1 PID Controller Parameters

In the CO₂ cycle, two PID controllers are employed to regulate the expansion valve opening and compressor speed. The PID controller used to regulate the shaft speed is implemented as depicted in Figure 3.8. For the compressor speed controller, a trial and error method was used to find the optimal parameter values, resulting in the following parameters:

$$\begin{aligned}K_p &= 1000 \\K_i &= 2 \\K_d &= 0\end{aligned}$$

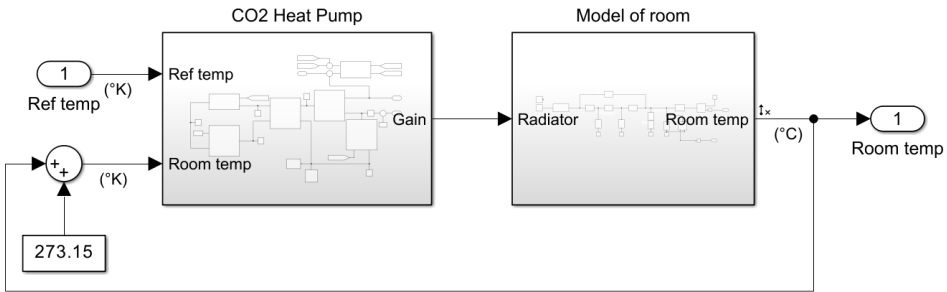


Figure 5.3: Simulink model of CO₂ heating cycle with heating facility

Here, the manipulated variable is the compressor speed, and the controlled variable is the room temperature.

In contrast, tuning the parameters of the expansion valve, which regulates the superheat in the vapor, was deemed unnecessary. Details about the expansion valve were discussed in Chapter 3. The valve controller parameters utilized were the same as those employed in the Matworks example model:

$$\begin{aligned}K_p &= 0.01 \\K_i &= 0.0001 \\K_d &= 0\end{aligned}$$

5.2.2 MPC Controller Parameters

The implementation of the MPC controller is depicted in Figure 5.4, where the manipulated variable is the compressor speed and the controlled variable is the room temperature. The selection of scale factors, penalty weights, sample time, and horizons for this implementation follows the same approach as used in Section 5.1.2 when choosing these parameters for the simplified radiator model.

Scale Factors

The input and output variables for the MPC controller used to regulate the compressor in the CO₂ heating cycle were scaled to have the following values:

$$\begin{aligned}\text{MV: } &6000 \\ \text{MD: } &1 \\ \text{MO: } &5\end{aligned}$$

Tuning Weights

The penalty weights on the inputs and outputs on the controller were determined to be:

$$\begin{aligned}\text{MV: } &1 \\ \text{MO: } &20\end{aligned}$$

Sample Time and Horizons

The sample time, prediction horizon and control horizon for the MPC controller were selected to be:

Sample time: 50
Prediction horizon: 20
Control horizon: 10

Constraints

A lower limit of 0 rpm and an upper limit of 6000 rpm were set as the constraints on the manipulated input variable in the controller.

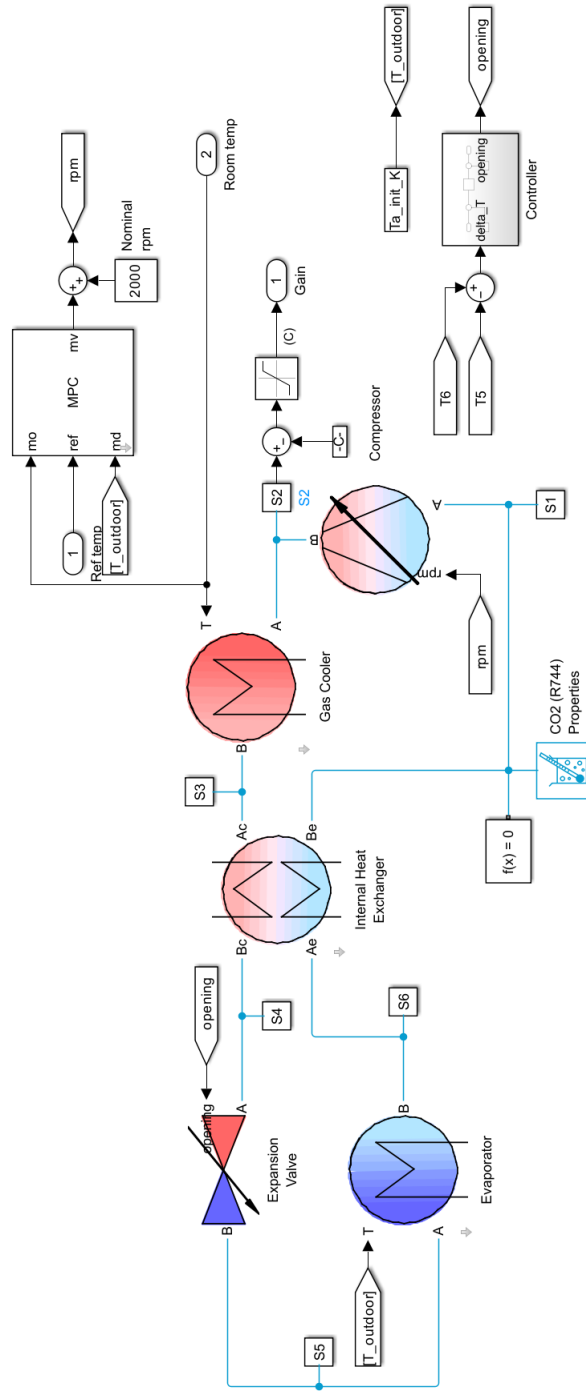


Figure 5.4: Simulink model of the CO₂ heating cycle with MPC control

6

Results

In this thesis, a CO₂ heat pump and a connected heating facility have been modeled, and the temperature development of the facility has been regulated using PID and MPC controllers. The aim of the study was to compare the performance of the two controllers in terms of their ability to maintain the desired temperature setpoint of the heating facility. The simulation was carried out using a dynamic model of the heating facility and the CO₂ heat pump system, which was developed based on the first principles of thermodynamics and fluid mechanics. The results of the simulation will now be analyzed and compared to determine the effectiveness of the PID and MPC controllers in controlling the temperature of the heating facility, and to evaluate the overall performance of the CO₂ heat pump system.

To obtain comparative data for the two controllers, the same setpoint is used for the different cases. Specifically, a step response of the set point temperature changes the temperature from 20 to 22°C after 30 minutes. The initial temperature of the room is set to 18°C for all simulations. Additionally, the radiator used in the simulations has an upper saturation limit of 100°C. This constraint is imposed by the physical properties of the system, as exceeding a temperature of 100°C would lead to an undesired phase change in the water.

6.1 Temperature Control Using the Simplified Radiator

In this section, the room model is connected to the simplified radiator. The controller output is equivalent to the temperature transferred from the radiator to the room.

6.1.1 Control of Temperature with PID

Figure 6.1 illustrates the temperature profile of the room and the corresponding PID controller output. The setpoint temperature increases from 20 to 22°C, and the controller increases the radiator temperature to the upper limit of 100°C for about five minutes before decreasing. The controller results in a relatively fast response with minimal oscillations

in the temperature. Although the initial rise time is quite slow, the plot demonstrates that the integral action in the controller eventually brings the room temperature to the setpoint. The controller requires nearly 30 minutes to reach the 20°C setpoint, which is expected given the large time constants typical of such systems.

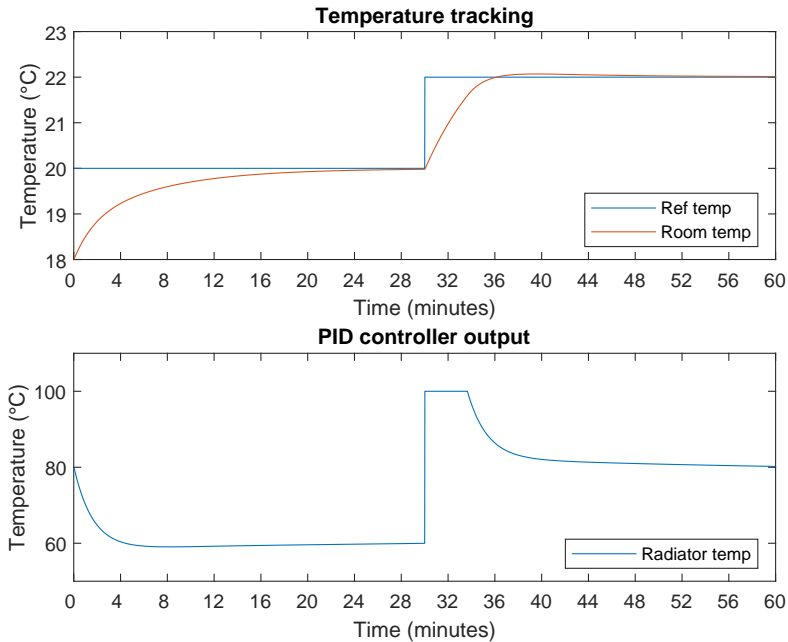


Figure 6.1: Step response of the development of the room temperature over one hour using a PID controller to control the radiator temperature. ($K_p = 40$, $K_i = 0.1$, $K_d = 0$)

6.1.2 Control of Temperature with MPC

The results of simulating the temperature development using MPC are plotted in Figure 6.2. The MPC controller is designed to minimize the difference between the desired and actual room temperature while considering the system's dynamics and the constraints on the control inputs. The same step response as for the PID controller (Figure 6.1) is also used for the MPC. For the room temperature to reach the initial setpoint of 20°C, the control output (radiator) reaches the maximum value of 100°C for a short duration before it drops down to 60°C. Right after the step response causes an increase in the setpoint, the controller output increases so that the room temperature approaches the new setpoint. It takes right under five minutes for the system to reach the new setpoint. Once the room temperature approaches the setpoint, the controller output is reduced but is still significantly higher than that for a setpoint of 20°C. The results indicate that the MPC controller effectively maintains the room temperature within a narrow range around the setpoint, outperforming the PID controller in terms of accuracy, rise time, and overshoot.

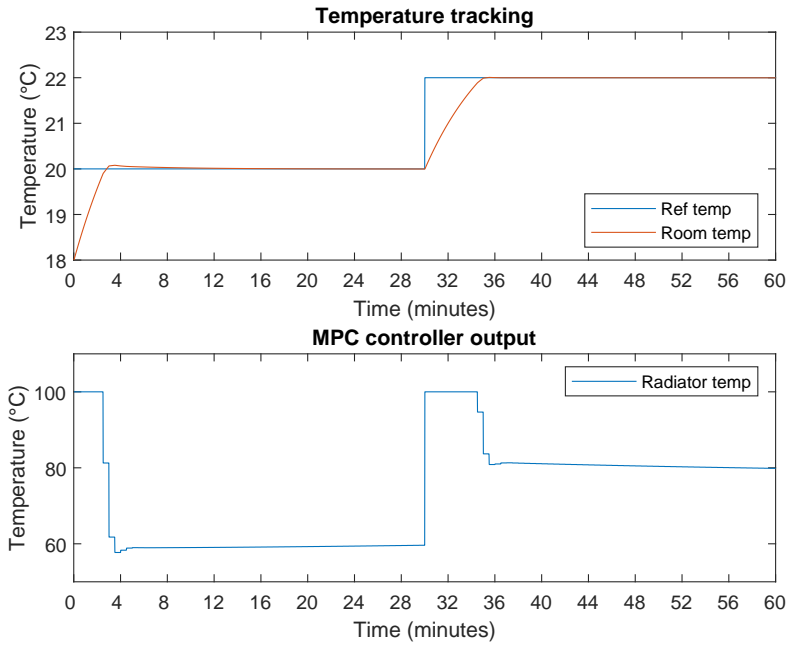


Figure 6.2: Step response of the development of the room temperature over one hour using MPC to control the radiator temperature.

6.2 Temperature Control with the CO₂ Cycle

In this section, the simulation results using the transcritical CO₂ heating cycle with PID and MPC control are presented.

6.2.1 PID Control of the Room Temperature

Figure 6.3 illustrates how the controller output changes to track the desired setpoint temperature. Initially, the room temperature is at 18°C but approaches the reference temperature of 20°C. After 30 minutes, the setpoint temperature is increased to 22°C, which causes the compressor's shaft speed to increase. As a result, the radiator temperature rises, which in turn increases the room temperature to the new setpoint. It takes approximately 12 minutes for the system to reach the new setpoint temperature.

It is important to note that the sudden jump in compressor speed after 30 minutes is not feasible in the physical system. In reality, the increase in compressor speed would be a gradual and controlled ramp-up process.

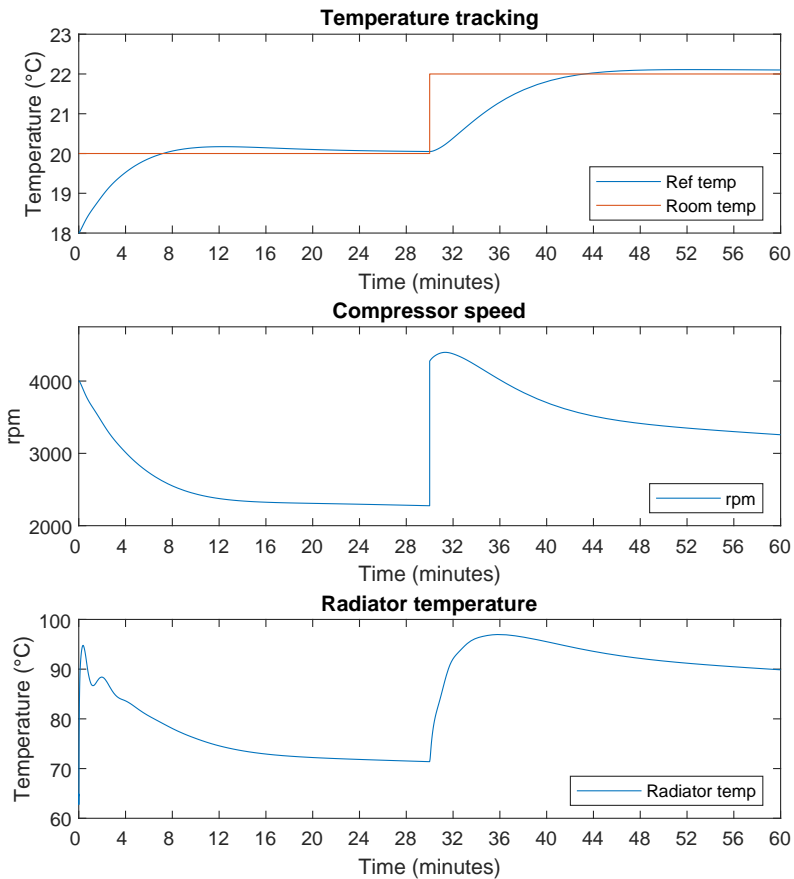


Figure 6.3: Step response of the development of the room temperature over one hour using PID to control the shaft speed of the compressor. ($K_p = 1000$, $K_i = 2$, $K_d = 0$)

6.2.2 Control of Room Temperature with MPC

Figure 6.4 displays the temperature development, compressor speed, and radiator temperature of the CO₂ heat pump and heating facility using MPC. The results indicate that the performance of the MPC controller is precise and accurate. The compressor speed is high, reaching the maximum of 6000 rpm, and resulting in a radiator temperature that saturates at 100°C. These results highlight the superior controller performance of the MPC compared to the PID and will be discussed in the following chapter.

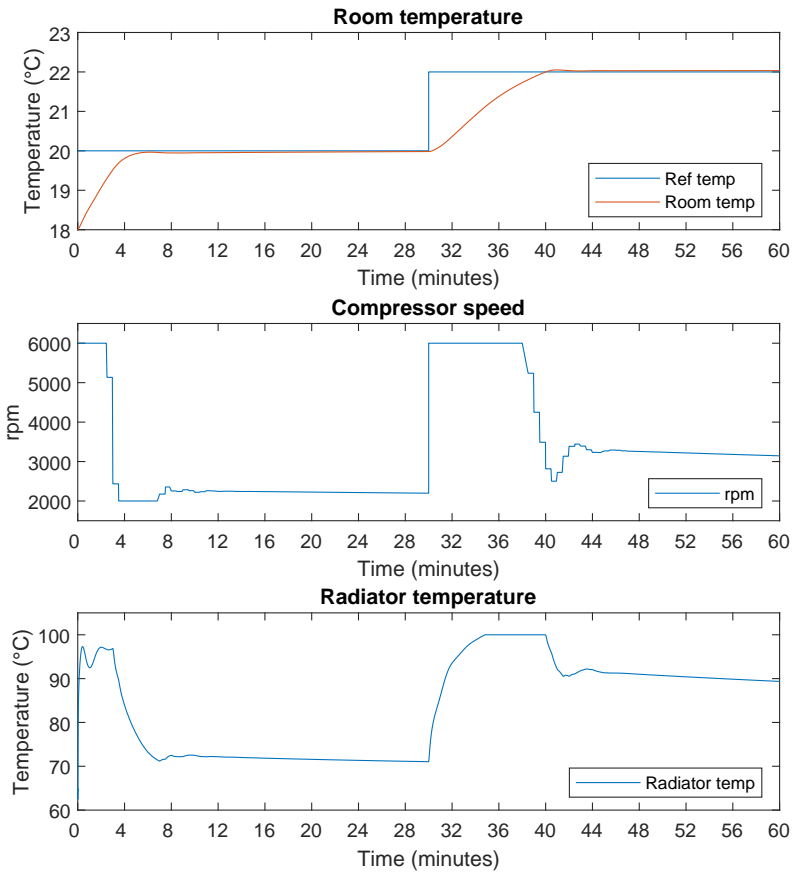


Figure 6.4: Step response of the development of the room temperature over one hour using an MPC controller to control the compressor speed.

7

Discussion

The discussion chapter aims to analyze and interpret the results obtained from the modeling and simulation of a CO₂ heat pump and its connected heating facility, with a focus on comparing the effectiveness of PID and MPC control strategies in regulating the temperature within the facility. By simulating the temperature development using two models - a simple radiator model and a more complex CO₂ heat pump model, the effectiveness of the two control methods can be analyzed. The results of this study provide important insights into the effectiveness of the two control methods for regulating room temperature in a heating facility. The findings indicate that while both control methods can achieve desired setpoint temperatures, the MPC method exhibits superior performance in terms of maintaining a desired temperature, but is more complicated to implement.

7.1 Controller Comparison

In this discussion section, the PID and MPC control strategies are compared and contrasted in terms of their performance, applicability, and implementation complexity. Specifically, the advantages and disadvantages of each method, the trade-offs between their performance metrics, and the factors that affect their selection and implementation in different applications are discussed.

The results of simulating the room temperature development with the two models suggest that the MPC controller is more effective than the PID controller in controlling the temperature. It is evident that the two MPC controllers had better setpoint tracking, less overshoot, and a smaller settling time, as observed in Figures 6.2 and 6.4. Although the MPC controllers are suited for applications where precise temperature control is critical, the PID controller may be better suited for temperature control in residential homes due to their ease of implementation and decent setpoint tracking.

Several strengths and weaknesses of both the PID and MPC controllers were identified. One of the main strengths of the PID controller is its simplicity and ease of implementation. It also has a well-established tuning methodology and can handle linear systems well. The main weakness of the PID controller is that it can be sensitive to changes in

the system, especially in the presence of nonlinearities and disturbances. In contrast, the MPC controller has a more complex structure, but it can handle nonlinear systems and disturbances more effectively, as observed when simulating the temperature development of the CO₂ cycle in Section 6.2. MPC also allows for the inclusion of constraints, which is critical for some applications. However, the MPC controller requires more computational resources, and the tuning process is more complex.

Considering the specific context of using controller to regulate the temperature of residential homes, the PID controller emerges as a more suitable choice based on the study's findings. In Figure 6.3, the measured temperature overshoots the reference with approximately 0.2°C, this overshoot does arguably not impact the comfort of room occupants. While the MPC controller outperformed the PID controller in terms of accuracy and rise time, the advantages of the PID controller, including its simplicity and ease of implementation, are more aligned with the requirements of residential temperature control, where precise and rapid adjustments are less critical.

These findings have significant implications for temperature control in various settings. In applications that require precise and robust temperature control, such as in hospitals, laboratories, and clean rooms, the MPC controller may be a better choice due to its superior accuracy and stability. However, the complexity and computational resources required by the MPC controller may limit its use in certain applications. On the other hand, for applications where a very high level of temperature control accuracy and stability is not critical, such as in residential homes, the simplicity and ease of implementation of the PID controller make it a more practical and cost-effective choice. The results highlight the importance of choosing the appropriate controller based on the specific application requirements and the trade-off between performance and complexity.

7.2 Limitations

As in most scientific research, it is important to recognize the constraints and possible sources of error that may have impacted the validity and generalization of the results. This section highlights the limitations of the project and the factors that may have influenced the results.

7.2.1 Simplified Assumptions

The modeling and simulations are based on certain assumptions and simplifications to make the analysis feasible. These assumptions may not capture all the complexities and nuances of the real system, leading to limitations in the accuracy and applicability of the results.

Room Model

The room model used in the simulation is based on mathematical equations that describe the physical laws of the universe. While mathematical modeling is a powerful tool for understanding complex systems and predicting their behavior under different conditions, it is important to recognize the limitations of mathematical models and the assumptions

on which they are based. Using the laws of physics to build models involves making simplifications that may not perfectly capture the real-world complexities of the physical system. It is crucial to recognize that mathematical models only work as approximations of the real system, and validating the models against empirical data should be done whenever possible.

A handful of assumptions were also made to simplify the modeling process. The assumptions include:

- The room is considered to be perfectly mixed, with uniform temperature and airflow throughout the room.
- Heat transfer between the external environment and the room occurs only through the walls, ceiling, and floor.
- Heat sources inside the room such as people and lighting are neglected.
- The effects of humidity, air quality, and radiation are neglected.

Assuming that the temperature inside the room is uniform is arguably the largest assumption made in the room model, and may be problematic as it does not reflect the real-life conditions resulting in inaccurate or unreliable simulations. However, since it is desired to have a simple model that is easy and fast to simulate, assuming a uniform temperature was deemed necessary in this project. It is, nevertheless, important to consider the potential limitations and inaccuracies of this assumption.

Heat Exchanger

Although assumptions are essential for simplifying systems, some simplifications can eliminate crucial dynamics from the model and are not always ideal. The heat exchange between the water loop and the CO₂ cycle in the heating facility is a case where the simplification likely removed important information and dynamics from the model. Figure 7.1 illustrates the simplification made in the heat exchange. The simplification assumes that the radiator gain, represented by the `Gain` label, is constantly 20°C lower than the hot CO₂ stream entering the gas cooler. However, in reality, the gas cooler is a heat exchanger, as discussed in Chapter 2. By simplifying the room temperature and gain as physical signals (e.g. a regular Simulink signal), the stream does not include flow rates or other thermal properties of the stream. This simplification makes it impossible to determine the actual temperature exchange between the CO₂ and water stream, thus removing essential information from the model.

7.2.2 Considerations for Controller Parameter Selection

During this project, having a quick controller was desired so that the room temperature quickly reached the setpoint. Having the controller parameters set to an aggressive response will, however, introduce more wear and tear on the physical system. Components such as valves and compressors have a limited lifespan and running these aggressively will likely require more maintenance and more frequent replacements. The potential wear and tear on the system has not been taken into account during control design in this project but should be investigated and considered when designing controllers on the physical system.

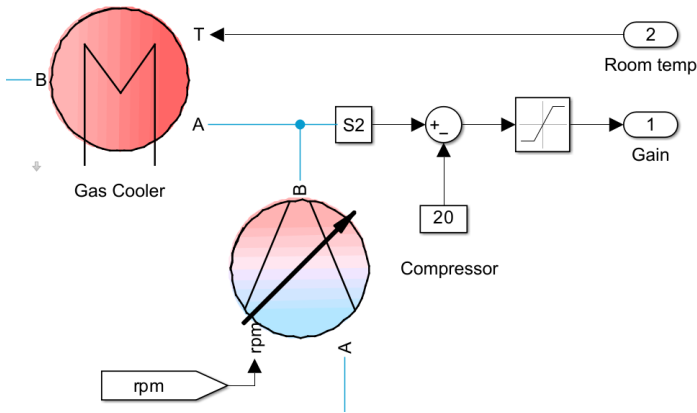


Figure 7.1: Simulink model of the simplified heat exchange between the CO₂ cycle and the water loop heating up the room

7.2.3 Equipment Sizing

The sizing of equipment used in the simulations does not accurately reflect the actual system's size or specific conditions. This can introduce uncertainties and potential discrepancies between the simulated and real-world performance. The limitations due to equipment sizing stem from challenges such as the availability and accuracy of data, the complexity of the models, uncertainties in load estimation, considerations of system interactions, and capturing the dynamic nature of the system. Accurate equipment sizing requires detailed information and coordination between components to ensure optimal performance. However, the lack of precise data, simplified modeling assumptions, and the dynamic behavior of the system can impact the accuracy of sizing decisions. Addressing these limitations is important for the reliability of the results, but as mentioned in Section 1.4 about delimitations, the models are made general, hence having the correct equipment sizing is therefore not emphasized in this project.

7.2.4 Generalizability

The research of this study focuses on the temperature control of a specific building, which limits the generalizability of the findings to other buildings or systems. Although the mathematical models used to describe the system have general applicability, the simulations rely on constants and parameters specific to the heating facility under investigation. As a result, factors like building design, climate conditions, and operational parameters differ across buildings, which can limit the transferability of the study's results.

8

Conclusion

In this project, a CO₂ heating cycle and its connected heating facility have been modeled and simulated, and the facility's temperature has been controlled. The simulations of the system were conducted using Matlab and Simulink, employing a mathematical model based on RC modeling principles to represent the facility. Two types of models were simulated: a simplified model of the radiator and a more complex model encompassing the entire transcritical CO₂ heating cycle. Both PID and MPC control strategies were applied to the simulations, allowing for a comparative analysis of the two controllers. Through the simulations, it was observed that both controllers exhibited distinct advantages and limitations in maintaining the desired room temperature. The PID controller demonstrated simplicity and ease of implementation, while the MPC controller showcased enhanced performance in terms of quick and accurate temperature regulation.

The findings of this thesis contribute to the understanding of control strategies for room temperature management. The comparison between PID and MPC controllers highlights the importance of considering factors such as system dynamics, disturbances, and control objectives when selecting an appropriate control strategy. Additionally, the specific application requirements play a crucial role in controller selection. While MPC excels in precise temperature control, PID control may be better suited for temperature control in residential homes.

While this study focused on the specific CO₂ heat pump and heating facility located in the laboratory at the Department of Energy and Process Engineering at NTNU, the insights gained from this study have broader implications. The models and methodologies developed can be applied to various HVAC systems, facilitating more informed decision-making and optimizing energy consumption in buildings.

8.1 Further Work

Although this study provides valuable insights into the behavior of the system under different control configurations, there are several areas that could be addressed in future work

to improve the models and the performance of the controllers. In this section, an outline of some of the potential avenues for future research are presented.

To improve the room model presented in Section 3.4, it is crucial to validate it using empirical data. By comparing the model output with actual data from the sensors on the heating facility in the laboratory, any discrepancies can be identified and the model can be refined for better accuracy.

Expanding the room model to incorporate various disturbances, such as occupancy patterns, appliance usage, and outdoor temperature changes, is essential to evaluate the robustness of the controllers. Additionally, investigating the scalability of the proposed control strategies to larger buildings or multiple zones will help identify challenges that arise when scaling up the control system and propose solutions to address them.

Lastly, the implementation of controllers on the physical system remains to be done. The thesis is delimited to only focus on the modeling of the heating cycle and facility, and simulation of the temperature development inside the facility under different control configurations. Implementation of the controllers is therefore mentioned here as further work.

Bibliography

- [1] U.S. Energy Information Administration, “2009 Residential Energy Consumption Survey Data,” 2012. [Online]. Available: <https://www.eia.gov/consumption/residential/data/2009/>
- [2] I. H. Magnussen, T. Ericson, A. Fidje, J. E. Fonnelløp, B. Langseth, W. W. Rode, and B. Saugen, *Varmepumper i energisystemet*, 2016. [Online]. Available: http://publikasjoner.nve.no/rapport/2016/rapport2016_{_}60.pdf
- [3] U. N. E. Programme, “Montreal protocol,” 1987, international treaty banning the production and consumption of ozone-depleting substances, including refrigerants such as chlorofluorocarbons and hydrochlorofluorocarbons. [Online]. Available: <https://ozone.unep.org/treaties/montreal-protocol-substances-deplete-ozone-layer>
- [4] R. U. Rony, H. Yang, S. Krishnan, and J. Song, “Recent advances in transcritical CO₂ (R744) heat pump system: A review,” *Energies*, vol. 12, 1 2019.
- [5] P. Neksa, “CO₂ heat pump systems,” *International Journal of Refrigeration*, vol. 25, 2002. [Online]. Available: www.elsevier.com/locate/ijrefrig
- [6] G. Achterbosch, P. de Jong, C. Krist-Spit, S. van der Meulen, and J. Verberne, “The development of a convenient thermal dynamic building model,” *Energy and Buildings*, vol. 8, no. 3, pp. 183–196, 1985. [Online]. Available: <https://www.sciencedirect.com/science/article/pii/0378778885900039>
- [7] G. Lefebvre, “Modal-based simulation of the thermal behavior of a building: the m2m software,” *Energy and Buildings*, vol. 25, no. 1, pp. 19–30, 1997. [Online]. Available: <https://www.sciencedirect.com/science/article/pii/S037877889600984X>
- [8] T. A. Mara, F. Garde, H. Boyer, and M. Mamode, “Empirical validation of the thermal model of a passive solar cell test,” 2012. [Online]. Available: <https://arxiv.org/abs/1212.3926>
- [9] C. Underwood, “An improved lumped parameter method for building thermal modelling,” *Energy and Buildings*, vol. 79, pp. 191–201, 2014. [Online]. Available: <https://www.sciencedirect.com/science/article/pii/S0378778814003831>

-
- [10] Y. Zhou, X. Zhou, J. Wang, and J. Yang, "Fuzzy control for compressor of co2 heat pump water heater based on digital signal controller," *ICIC Express Letters, Part B: Applications*, vol. 9, pp. 1249–1256, 12 2018.
- [11] M. Kasahara, T. Matsuba, Y. Kuzuu, T. Yamazaki, and e. al, "Design and tuning of robust pid controller for hvac systems," *ASHRAE Transactions*, vol. 105, p. 154, 1999.
- [12] J. Clauß and L. Georges, "Model complexity of heat pump systems to investigate the building energy flexibility and guidelines for model implementation," *Applied Energy*, vol. 255, 12 2019.
- [13] A. Wang, X. Yin, J. Fang, F. Jia, Y. Song, and F. Cao, "A novel frost-free control strategy and its energy evaluation of the co2 heat pump system," *Applied Thermal Engineering*, vol. 201, 1 2022.
- [14] H. Kim, Y. Yoon, Y. Cho, and M. Kim, "Model predictive control for residential heat pump system based on adaptive disturbance observer," *Applied Energy*, vol. 239, pp. 412–421, 2019.
- [15] J. Yang, S. Yang, X. Hu, Q. Jin, and J. Liu, "A model predictive control strategy for a variable refrigerant flow heat pump system," *Sustainability*, vol. 11, p. 6354, 2019.
- [16] J. Drgoña, J. Arroyo, I. Cupeiro Figueroa, D. Blum, K. Arendt, D. Kim, E. P. Ollé, J. Oravec, M. Wetter, D. L. Vrabie, and L. Helsen, "All you need to know about model predictive control for buildings," *Annual Reviews in Control*, vol. 50, pp. 190–232, 2020. [Online]. Available: <https://www.sciencedirect.com/science/article/pii/S1367578820300584>
- [17] D. Picard, F. Jorissen, and L. Helsen, "Methodology for obtaining linear state space building energy simulation models," *Proceedings of the 11th International Modelica Conference, Versailles, France, September 21-23, 2015*, vol. 118, pp. 51–58, 9 2015.
- [18] M. Castilla, J. Álvarez, J. Normey-Rico, and F. Rodríguez, "Thermal comfort control using a non-linear mpc strategy: A real case of study in a bioclimatic building," *Journal of Process Control*, vol. 24, no. 6, pp. 703–713, 2014, energy Efficient Buildings Special Issue. [Online]. Available: <https://www.sciencedirect.com/science/article/pii/S0959152413001819>
- [19] F. Jorissen, D. Picard, I. Cupeiro Figueroa, W. Boydens, and L. Helsen, "Towards real mpc implementation in an office building using taco," in *International High Performance Buildings Conference*. Purdue, 2018.
- [20] R. M. Santos, Y. Zong, J. M. C. Sousa, L. Mendonça, and A. Thavlov, "Nonlinear economic model predictive control strategy for active smart buildings," in *2016 IEEE PES Innovative Smart Grid Technologies Conference Europe (ISGT-Europe)*, 2016, pp. 1–6.
- [21] A. Bhattacharya, X. Ma, and D. Vrabie, "Model predictive control of discrete-continuous energy systems via generalized disjunctive programming," 2020.

-
- [22] A. Afram and F. Janabi-Sharifi, "Theory and applications of hvac control systems – a review of model predictive control (mpc)," *Building and Environment*, vol. 72, pp. 343–355, 2014. [Online]. Available: <https://www.sciencedirect.com/science/article/pii/S0360132313003363>
- [23] D. Q. Mayne, "Model predictive control: Recent developments and future promise," *Automatica*, vol. 50, no. 12, pp. 2967–2986, 2014. [Online]. Available: <https://www.sciencedirect.com/science/article/pii/S0005109814005160>
- [24] M. Kvasnica, B. Takács, J. Holaza, and S. Di Cairano, "On region-free explicit model predictive control," in *2015 54th IEEE Conference on Decision and Control (CDC)*, 2015, pp. 3669–3674.
- [25] E. L. Cosgriff, "Optimal control of a co2 heat pump with a heating facility," 2022.
- [26] S. A. Kalogirou, *Solar Energy Engineering*, second edition ed., Boston, 2014. [Online]. Available: <https://www.sciencedirect.com/science/article/pii/B9780123972705000054>
- [27] O. Levenspiel, *Engineering Flow and Heat Exchange*, 3rd ed. New York, NY: Springer, 2014.
- [28] J. R. Welty, G. L. Rorrer, D. G. Foster, and C. E. Wicks, *Fundamentals of Momentum, Heat and Mass Transfer*, 5th ed. John Wiley amp; Sons, Inc., 2008.
- [29] R. A. Otón-Martínez, F. Illán-Gómez, J. R. García-Cascales, F. J. Velasco, and M. R. Haddouche, "Impact of an internal heat exchanger on a transcritical co2 heat pump under optimal pressure conditions: Optimal-pressure performance of co2 heat pump with ihx," *Applied Thermal Engineering*, vol. 215, 10 2022.
- [30] Y. Li, N. Nord, H. Halvorsen, and I. H. Rekstad, "Model-based sizing of a co2 heat pump for residential use," *Sustainable Energy Technologies and Assessments*, vol. 53, 2022.
- [31] M. S. Kim, C. S. Shin, and M. S. Kim, "A study on the real time optimal control method for heat rejection pressure of a co2 refrigeration system with an internal heat exchanger," *International Journal of Refrigeration*, vol. 48, pp. 87–99, 2014.
- [32] P. Neksfitt, H. Rekstad, G. R. Zakeri, and P. A. Schiefloe, "Co2-heat pump water heater: characteristics, system design and experimental results*," *International Journal of Refrigeration*, vol. 21, pp. 172–179, 1998.
- [33] D. E. Seborg, T. F. Edgar, D. A. Mellichamp, and F. J. Doyle, *Process Dynamics and Control*, 3rd ed. JOHN WILEY amp; Sons, 2011.
- [34] B. Sohlberg, *Grey Box Modelling*. London: Springer London, 1998, pp. 7–43. [Online]. Available: https://doi.org/10.1007/978-1-4471-1558-8_2
-

-
- [35] G. Reynders, J. Diriken, and D. Saelens, "Quality of grey-box models and identified parameters as function of the accuracy of input and observation signals," *Energy and Buildings*, vol. 82, pp. 263–274, 2014. [Online]. Available: <https://www.sciencedirect.com/science/article/pii/S0378778814005623>
- [36] S. Chandra, M. K. Sharma, and M. Sharma, *Conservation Laws*. Foundation Books, 2014, p. 60–119.
- [37] B. R. Sørensen and V. Novakovic, "Dynamisk modellering og simulering av klimasystemer," 1995.
- [38] C. Stanciu, D. Stanciu, and A.-T. Gheorghian, "Thermal analysis of a solar powered absorption cooling system with fully mixed thermal storage at startup," *Energies*, vol. 10, p. 72, 01 2017.
- [39] G. Towler and R. Sinnott, *Chemical Engineering Design*, second edition ed. Butterworth-Heinemann, 2013. [Online]. Available: <https://www.sciencedirect.com/science/article/pii/B9780080966595000171>
- [40] S. Skogestad and C. Grimholt, "The simc method for smooth pid controller tuning," *Advances in Industrial Control*, pp. 147–175, 01 2012.
- [41] S. Qin and T. A. Badgwell, "A survey of industrial model predictive control technology," *Control Engineering Practice*, vol. 11, no. 7, pp. 733–764, 2003. [Online]. Available: <https://www.sciencedirect.com/science/article/pii/S0967066102001867>
- [42] A. Bemporad, N. L. Ricker, and M. Morari, "Model predictive control toolbox™ getting started guide," 2022. [Online]. Available: https://se.mathworks.com/help/mpc/index.html?s_tid=srchtitle_model%20predictive%20control%20toolbox_1
- [43] Engineering ToolBox, "Heat loss from buildings," 2003. [Online]. Available: https://www.engineeringtoolbox.com/heat-loss-buildings-d_113.html
- [44] J. G. Ziegler and N. B. Nichols, "Optimum settings for automatic controllers," *ASME*, vol. 64, 1942.
- [45] J. G. Balchen, T. Andresen, and B. A. Foss, *Reguleringsteknikk*, 6th ed. Institutt for teknisk kybernetikk, 2016.
- [46] M. L. Luyben and W. L. Luyben, *Essentials of Process Control*. THE MCGRAW-HILL COMPANIES, INC., 1997.
- [47] S. Skogestad, "Simple analytic rules for model reduction and pid controller tuning," 2003. [Online]. Available: www.elsevier.com/locate/jprocont

Appendix

A Matlab files

Constants

```
1 % Room dimensions
2 height_room = 2.5;           % m
3 lenght_wall = 3;           % m
4 debth_wall = 3;           % m
5 thickness_external_wall = 0.15; % m
6 thickness_internal_wall = 0.15; % m
7 thickness_ceiling = 0.2;     % m
8 thickness_floor = 0.2;      % m
9
10
11 % Area
12 area_wall = height_room*lenght_wall; % m^2
13 area_ceiling = lenght_wall*debth_wall; % m^2
14 area_window = height_room*lenght_wall; % m^2
15 area_external_wall = height_room*lenght_wall; % m^2
16 area_external_roof = lenght_wall*debth_wall; % m^2
17 area_floor = lenght_wall*debth_wall; % m^2
18
19
20 % Volume
21 room_volume = height_room*lenght_wall*debth_wall; %m3
22 external_wall_volume = height_room*lenght_wall*thickness_external_wall;%m3
23 internal_wall_volume = height_room*lenght_wall*thickness_internal_wall;%m3
24 ceiling_volume = lenght_wall*debth_wall*thickness_ceiling; %m3
25 floor_volume = lenght_wall*debth_wall*thickness_floor; %m3
26
27
28 % Physical values
29 rho_air = 1.2; % kg/m^3
30 cp_air = 1012; % J/(kg*K)
31
32 cp_external_wall = 2700*0.2+1030*0.8; % J/(kg*K) assuming wall is 20%
    wood and 80% insulation
33 rho_external_wall = 500*0.2+31*0.8; % kg/m^3 assuming wall is 20% wood
    and 80% insulation
34 cp_internal_wall = 2700*0.2+1030*0.8; % J/(kg*K)
35 rho_internal_wall = 500*0.2+31*0.8; % kg/m^3
36 cp_ceiling = 2700*0.2+1030*0.8; % J/(kg*K)
37 rho_ceiling = 500*0.2+31*0.8; % kg/m^3
38 cp_floor = 2700*0.2+1030*0.8; % J/(kg*K)
39 rho_floor = 500*0.2+31*0.8; % kg/m^3
40
41
42 % Radiator
43 radiator_heat_effect = 2000; % W
44
```

```

45
46 % Convective heat transfer coefficients
47 htc_wall_air = 3;           % W/(m^2*K)
48 htc_window_wall = 5;      % W/(m^2*K)
49 htc_window_air = 3;       % W/(m^2*K)
50 htc_rad = 7;              % W/(m^2*K)
51
52
53 % Overall heat transfer coefficients
54 U_external_wall = 0.7;    % W/(m^2*K)
55 U_external_roof = 2.2;   % W/(m^2*K)
56 U_floor = 3;             % W/(m^2*K)
57 U_window = 2.3;         % W/(m^2*K)
58
59
60 % Resistance
61 R_external_wall = 1/(area_external_wall*U_external_wall);
62 R_external_roof = 1/(area_external_roof*U_external_roof);
63 R_floor = 1/(area_floor*U_floor);
64 R_window = 1/(area_window*U_window);
65 Rconv_wall = 1/(htc_wall_air*area_wall);
66 Rconv_rad = 5*(60)/(radiator_heat_effect);
67
68
69 % Capacitance
70 C_air = room_volume*cp_air*rho_air;
71 C_external_wall = external_wall_volume*rho_external_wall*cp_external_wall;
72 C_internal_wall = internal_wall_volume*rho_internal_wall*cp_internal_wall;
73 C_floor = floor_volume*rho_floor*cp_floor;
74 C_ceiling = ceiling_volume*rho_ceiling*cp_ceiling;

```

Initialization

```

1  clc
2  close all
3  clear all
4
5  % Initial temperatures
6  Ta_init = 5;           % C
7  Ti_init = 18;         % C
8  Tg_init = 18;         % C
9  Tz_init = 18;         % C
10 Ta_init_K = Ta_init + 273.15; % K
11
12
13 % Load constants
14 run constants;
15
16 % Open and run the transcritical CO2 cycle needed to load CO2 properties
17 open ssc_transcritical_refrigeration;
18 run ssc_transcritical_refrigeration;

```

B Modeling Ventilation and Infiltration

Ventilation and infiltration can impact a room's thermal behavior. While the heat loss through the surfaces has been modeled earlier, the modeling of heat loss from ventilation and infiltration remains to be added to the room model. It was chosen to not include ventilation and infiltration to keep the original model as simple as possible. This section, however, will explain how the room model may be expanded to include ventilation and infiltration.

Ventilation refers to the intentional exchange of indoor air with outdoor air, while infiltration refers to the unintentional exchange of air through leaks or cracks in the building envelope. Both processes can affect the room's temperature and humidity by introducing heat or moisture from outside. Most buildings do not have perfect insulation, and will often lose heat from transmission, ventilation, and infiltration. Although one could consolidate all these losses into a single heat transfer equation, it may be more clear to separate the heat loss due to ventilation and infiltration from the transmission heat losses. The equation for the overall heat loss due to ventilation and infiltration can be expressed as:

$$Q = Q_v + Q_i \quad (8.1)$$

where Q_v is the heat loss from ventilation, and Q_i is the heat loss from infiltration.

The heat loss from ventilation is expressed as:

$$Q_v = c_p \rho q_v \Delta T \quad (8.2)$$

where c_p denotes the specific heat capacity of air, ρ denotes the density of air, q_v denotes the volumetric flow of air, and ΔT denotes the temperature difference between the indoor and outdoor air. Some of the heat loss through ventilation is often recovered through the heat exchanger [43], this effect may be added to the mathematical expression. Equation 8.2 can be rewritten as:

$$Q_v = (1 - \beta/100) c_p \rho q_v \Delta T \quad (8.3)$$

where β denotes the heat recovery efficiency in percentage. For rooms equipped with air-air or water-air counterflow heat exchangers, the typical heat recovery efficiency is around 50% [43].

Infiltration heat loss occurs due to air leakage through construction cracks or gaps in doors and windows. Due to the complex nature of infiltration, exact modeling is challenging and depends on various factors such as temperature differences, wind speeds, and frequency of door openings and closures [43]. The heat loss through infiltration can be approximated using the following equation:

$$Q_i = c_p \rho n V \Delta T \quad (8.4)$$

where n represents the frequency of air replacement, i.e., how often the air is replaced, and V is the volume of the room. A commonly used value for n is 0.5 air changes per hour, which corresponds to $1.4 \times 10^{-4}/s$ [43].

C PID Tuning Methods

Ziegler-Nichols method

In 1942, Ziegler and Nichols introduced a method for tuning controllers known as the continuous cycling method or more commonly called the Z-N method [44]. This approach involves a trial-and-error process of identifying constants that cause the system to oscillate. To begin, the integral and derivative actions of the controller are disabled, leaving only the proportional action, and K_c is set to a small value such as 0.5. A small setpoint change is introduced to create an error between the setpoint and the controlled variable while the controller is in automatic mode. Gradually increasing the K_c value results in oscillations. The K_c value that produces stable oscillations with a constant amplitude and period is referred to as the ultimate gain, K_{cu} , while the period of oscillations is known as the ultimate period, P_u . The tuning relations for calculating the PID controller settings were published by Ziegler and Nichols and can be found in Table A.1.

Ziegler-Nichols	K_c	τ_I	τ_D
P	$0.5K_{cu}$	-	-
PI	$0.45K_{cu}$	$P_u/1.2$	-
PID	$0.6K_{cu}$	$P_u/2$	$P_u/8$

Table A.1: Tuning relations for the Z-N method [44]

Although widely used in industry [33] and considered a straightforward tuning method [45], the Z-N approach has certain limitations. One significant disadvantage is that the method necessitates the process to approach the stability limits, which can be hazardous if external disturbances or modifications to the process cause it to become unstable. Additionally, for systems with slow process dynamics, the trial-and-error procedure used to determine K_{cu} can be time-consuming. Z-N method is also known for producing quite aggressive controllers. If a more conservative controller is desired, the Tyreus-Luyben tuning relations can be used instead [46].

It remains uncertain whether Ziegler and Nichols initially devised the tuning approach for PID controllers in series or parallel form [33]. In the case of the CO₂ heat pump system, the PID controller is in parallel form, which will lead to a slightly more conservative controller when utilizing the Z-N method [47].

SIMC method

The SIMC approach shares many of the Z-N method's principles but is known to perform better on systems with time delays and is also effective for handling disturbances in setpoints and loads [40].

Before the tuning parameters are found, the SIMC method uses a model approximation to obtain a first-order-plus-time-delay model (FOPTD). The transfer function for a FOPTD can be expressed as:

$$\tilde{G}(s) = \frac{Ke^{-\theta s}}{\tau s + 1} \quad (8.5)$$

The controller can be represented by the following expression:

$$K_c = \frac{1}{K} \frac{\tau}{\theta + \tau_c} \quad (8.6)$$

One way to identify transfer function parameters is to fit a FOPTD model with an open-loop step response, which can be relatively simple. Other methods for fitting data also exist, such as using a proportional-only controller in a closed-loop setpoint response (e.g., the Z-N method) or utilizing a detailed model [40]. Nevertheless, this paragraph will focus exclusively on the open-loop step response method.

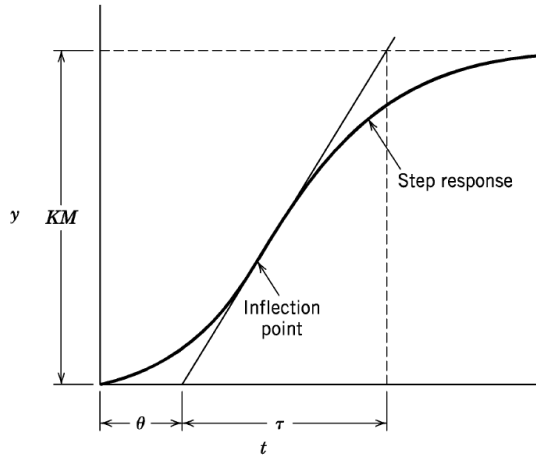
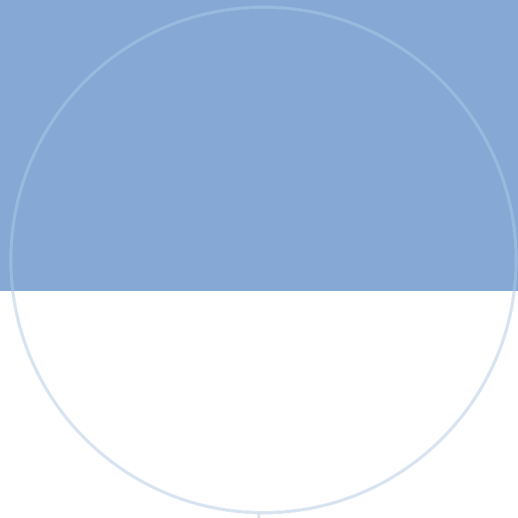
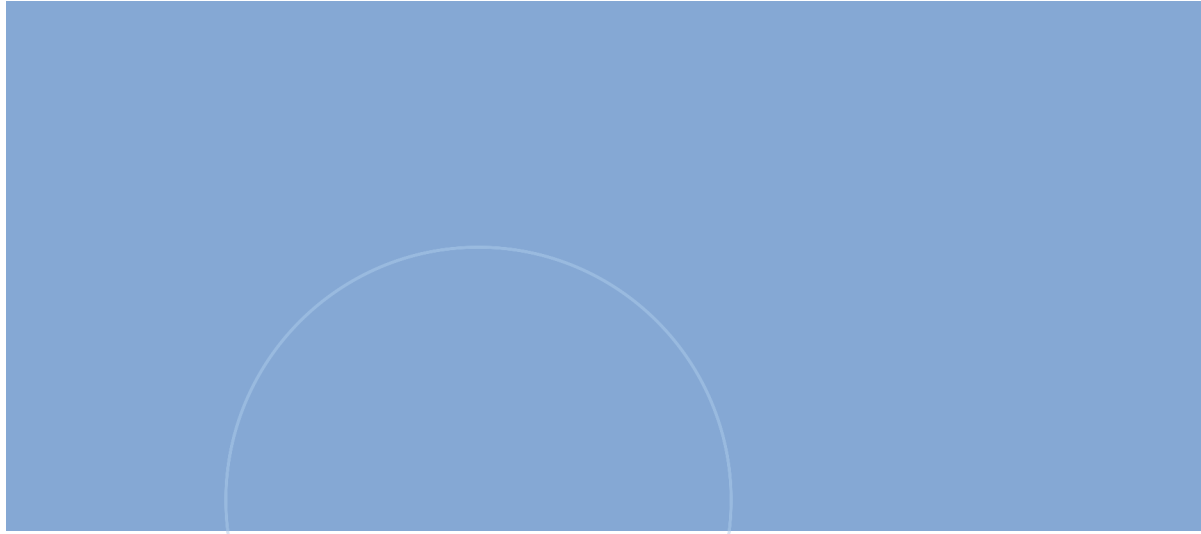


Figure 8.1: Process reaction curve for a first-order-plus-time-delay model [33]

To determine the transfer function parameters of a FOPTD model, graphical analysis of the process reaction curve (Figure 8.1) can be used. The ratio between the steady-state change and the input step change, M , represents the process gain K . To determine the time delay θ , the slope is taken at the inflection point and then intersected with the x -axis. Similarly, the tangent line is extended to the intersection point where $y = KM$ to find τ . Thus, the time constant can be calculated as $t = \theta + \tau$.

In the case of lag dominant processes, where the time constant is much greater than the time delay ($\tau \gg \theta$), it is important to reduce the integral time to avoid slow oscillations. According to Skogestad [47], the integral time should be set in such a way that slow oscillations are avoided. This can be achieved by setting the integral time τ to the minimum of τ and $4(\tau_c + \theta)$. To achieve tight control with a smooth response, it is recommended to set the reset time τ_c equal to the time delay θ . However, if the system has a small time delay, this can lead to an overly aggressive controller. To obtain a smoother controller, τ_c can be set greater than θ , and there is no upper limit to how large τ_c can be. However, Skogestad suggests a maximum value for τ_c given by $\tau_{c,max} = \frac{1}{K_{c,min}} \frac{\tau}{K} - \theta$, where $K_{c,min}$ is the minimum value of the controller gain that is required to reject a disturbance, and Δy_{max} is the maximum allowable deviation in the output.



 **NTNU**

Norwegian University of
Science and Technology